HHS Public Access

Author manuscript

Anal Chem. Author manuscript; available in PMC 2021 January 07.

Published in final edited form as:

Anal Chem. 2020 January 07; 92(1): 49–66. doi:10.1021/acs.analchem.9b04718.

Challenging Bioanalyses with Capillary Electrophoresis

Courtney J. Kristoff, **Lloyd Bwanali**, **Lindsay M. Veltri**, **Gayatri P. Gautam**, **Patrick K. Rutto**, **Ebenezer O. Newton**, **Lisa A. Holland***

C. Eugene Bennett Department of Chemistry, West Virginia University, Morgantown, West Virginia 26506, United States

Graphical Abstract

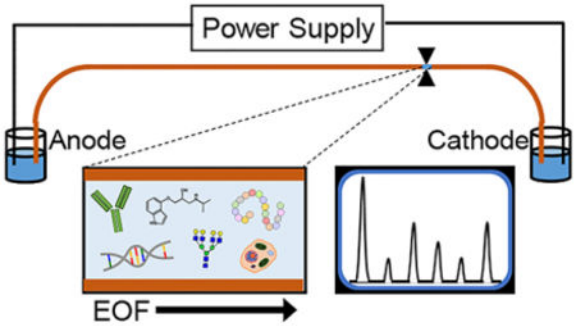

This report covers advances in capillary electrophoresis (CE) from January 2018 through September 2019. A summary of the literature during this time period is insightful. A search performed using the SciFinder Scholar® database for journal reports (limited to English) using the term capillary electrophoresis returned approximately 1,800 publications. Further analysis of this list, depicted in Figure 1, provided a snapshot of activity in biomolecular research. Classes of biomolecules most frequently associated with CE publications were proteins, drugs, DNA and metabolites. Another measure of the impact of CE is the translation of this technology into society. A search of patent activity illustrating this process of CE technology transfer returned 346 patents published in all languages, with a substantial contribution reported only in Chinese (198 patents) or English (98 patents). The versatility of CE for biological systems is exemplified by the rise of the technique in several areas. Metabolomics research involving measurements of large sets of molecules with subtle structural differences benefits from rapid separations achieved with high peak capacity and automated instruments. Single cell and sub-cellular analyses continue to progress in CE because of the size compatibility of the technique with the sample. Other examples of areas utilizing CE that are accelerating include portable and printable instrumentation, affinity interaction, as well as proteomics. As an established analytical tool, CE instrumentation and methods have been designed to be accessible and easily adopted by researchers with expertise in areas beyond the field of separations. Generally, publications including CE measurements either outline innovations in the technique or they are compelling applications of a mature analytical approach. The goal of this review, which is limited to 180 citations, is

*Corresponding author contact information: Lisa.Holland@mail.wvu.edu.

to communicate an overview of recent developments, focusing on reports describing advances to the technology. Although publications that utilize CE are found in a diverse set of periodicals, the reports included in this review are from journals that are popular in the field of analytically-based separation chemistry.

Several attributes of CE have led to the high rate of publications focused on biomolecules summarized in Figure 1. This includes rapid separation times, low sample volume requirements (e.g. nL) and reduced consumption of buffers. Although the simplest implementation of CE, free zone electrophoresis, is based solely on differences in charge-to-size ratio, CE platforms are versatile, accommodating other modes of separation through sieving and secondary equilibria (e.g. micelle partitioning, electrochromatography and host:guest complex formation). The unrivalled compatibility between biomolecular analyses and capillary electrophoresis is evidenced in the recent activities leveraging CE to search for molecular signatures of life beyond Earth.[1–4] While CE can be designed to be portable, it is also amenable to automation, making it appealing for high throughput measurement applications. In addition, the nature of CE creates some design considerations when interfacing the separation with different modes of detection. This separation technique continues to evolve. Previously unachievable analyses are emerging as new strategies are devised to mitigate barriers to realizing the full potential of the method. Instrumental advances reported during this time period included integrated systems and enhanced detection.

This review covers CE advances by biomolecular class according to the number of publications in the field. The discussion begins with proteins and progresses to pharmaceuticals, DNA, metabolites and finally carbohydrates. Reports on peptides and amino acids frequently overlapped with papers covered under the proteomics and metabolomics sections, and as a result a dedicated discussion of these molecular classes was not warranted. Instrumental advances relevant to a specific area are described according to molecular targets. At the conclusion of this review, emerging and evolving applications are highlighted as a vision for future directions in this field. Two recent reviews in this Journal overlap with some areas of biomolecular CE analyses and the reader is referred to these other sources for a thorough discussion of these topics. Although capillary gel electrophoresis is a widely used and accepted tool for DNA-based human identification in the criminal justice system, progress in this specific area has been thoroughly communicated in a recent fundamental review in this Journal.[5] Coverage of DNA applications in this review is limited to aptamers. Likewise, affinity binding measurements with capillary electrophoresis, which is a flexible platform to achieve measurements of biomolecular systems under a variety of conditions, is the subject of another excellent fundamental review in this Journal.[6] As much as possible, the article is written to accommodate active practitioners of CE in addition to researchers considering entering the field.

1. Proteins

Capillary electrophoresis is highly adaptive to protein separations. Proteins are among the most diverse class of physiologically relevant biomolecules. These biomolecules vary in net charge and size. Most are aqueous soluble. They are composed of isoforms and variants for

which these different forms display differences in function. Structure, post-translational modification, affinity binding, enzyme function and chemical reactions are all easily studied with different modes of capillary electrophoresis.

The versatility of CE for protein analyses is demonstrated in Figure 2 which displays two recently published separations of protein size standards. The top trace (Figure 2A) is a size-based sieving separation of proteins transported through a well packed colloidal silica capillary operated under electrophoresis.[7] The silica colloid is composed of particles of diameter 345 ± 10 nm. In the presence of the surfactant sodium dodecyl sulfate (SDS), the proteins acquire a similar charge- to-size ratio. The efficiency was reported in terms of plate height at a value of 0.53 μm. This corresponds to nearly 100,000 theoretical plates for a 5 cm separation distance. Both the efficiency achieved in this separation as well as the short run time are vastly superior to that achieved with polyacrylamide gels.

At the other extreme of separation science is the high throughput protein separation shown in Figure 2B. The separation is obtained in a microfluidic channel through size-based sieving of a protein ladder using SDS and a physical gel composed of an entangled linear polymer matrix.[8] A high field strength of 800 V/cm was used in the separation channel, which was 8.8 μm deep and only 3-mm long. The electropherogram appears unusually thick because it consists of 70 overlaid traces achieved with repetitive analyses in only 196 seconds. While the high throughput system does not achieve the peak resolution evident in Figure 2A, the speed of these sub-3 second separations enables remarkable throughput for protein analyses. This separation is integrated in a device capable of delivering sample in the form of a droplet train, creating an integrated platform for truly high throughput measurements of physiological systems.

Most capillary electrophoresis separations lie between these two extremes. For more conventional approaches to capillary sieving, improvement and assessment continued during the timeframe of this review. Different options available for commercial capillary electrophoresis systems were compared for 5 different vendors.[9] In addition, kits or recommended methods provided by the manufacturers were evaluated for the analytical figures of merit associated with size-based protein separations.[9] Similar to a “consumer report” this article provided insight regarding these instruments and the methods for protein separation associated with them in an effort to assist and inform researchers in need of this technology.[9] Other factors that impact protein sieving separations have been reported as well. Different variables associated with specific sieving materials such as concentration, applied field and separation length have also been described.[10] The generic role of buffers on separation current, adsorption and peak shapes obtained in protein separations was also examined with a special emphasis on the use of background electrolytes composed of different combinations of zwitterionic buffers.[11]

1.1 Capillary Coatings

One of the most pervasive barriers is the adsorption of proteins to the fused silica surface. Researchers can avoid this problem by using highly acidic background electrolyte to protonate the negatively charged fused silica surface; however, a consequence of acidic running buffer is the suppression of electroosmotic flow at low pH. This can adversely affect

separations of proteins with low isoelectric points, which will migrate quite slowly through the capillary. Alternatively, the surface of the separation capillary can be passivated through covalent modification,[12,13] physical adsorption,[14–18] or dynamic coatings. Several research reports emphasize surface coatings for protein separations, although in some cases surface passivation is described but not elaborated.

Covalently-modified capillaries have surfaces that do not require regeneration, but they can be expensive to purchase from commercial vendors and must be discarded if the surface becomes compromised. A photosensitive coating formed from diazotized poly (vinyl alcohol-*b*-styrene)(diazo-P(VA-*b*-St)) was designed to reduce protein adsorption and was demonstrated with a separation of bovine serum albumin, ribonuclease A and lysozyme.[12] The semi-permanent coating was rinsed through the capillary and then polymerized following exposure to UV light. Another report of a covalently-modified capillary was achieved through polymerization of a porous layer open-tubular capillary.[13] Carrier ampholytes were positioned in the capillary with isoelectric focusing and then polymerized to the surface. Two different immobilized pH gradients were generated. A narrow pH gradient (pH 4.5 to 6.0) as well as a wider pH gradient (pH 3 to 10) were evaluated using sets of 4 proteins with isoelectric points that were relevant to each pH gradient.

Physically-adsorbed coatings form through interactions of the coating reagent with the silica surface. Typically, the surface is regenerated between runs with a flushing protocol. This allows for a capillary with a compromised surface to be reused upon reapplication of the coating. A semi-permanent coating was developed for nanoparticle electrochromatography using multi-walled carbon nanotubes with different functionalization in conjunction with SDS.[16] Protein separated with the modified capillaries had separation efficiencies up to 23,000 plates/m using a background electrolyte buffered to a pH of 8.4. Another report utilized nanocrystals comprised of zeolite imidazolate framework-8 (ZIF-8) to separate 4 proteins of different isoelectric points using a background electrolyte buffered to pH of 3.[18] A different study described multilayer coatings comprised of polyelectrolytes to enable separations of proteins.[15] Using a 5-layer coating a stable positively charged surface was created that yielded high separation efficiencies for proteins using a background electrolyte buffered to 2.5. A semi-permanent coating created from a self-assembled phospholipid bilayer further modified to be cationic was used to simultaneously separate cationic and anionic proteins with high efficiency using background electrolytes buffered to pH values ranging from 4–9.[14] The hydrophobic tail of the cationic surfactant, cetyltrimethylammonium bromide, inserted into the phospholipid bilayer based on hydrophobic interactions. The modified surface had a stable reversed electroosmotic flow regardless of the pH of the background electrolytes between a range of 4–9 and proteins did not adsorb to the semi-permanent surface.

1.2 Proteomics

Proteomics is an active field of research providing insight into protein function and expanding the number of proteins identified in physiological systems. The gold standard for proteomics research is liquid chromatography coupled with mass spectrometry (LC-MS); however, CE provides complementary information to LC and is increasingly integrated with

chromatographic separations. CE also provides high resolution separations of complex mixtures. Moreover, CE is compatible with the small sample sizes associated with biological health-related research.

Multi-dimensional separation platforms that include CE highlight the increased separation capability achievable with this approach. By incorporating CE, the number of proteins and proteoforms identified in proteomics studies is significantly increased. A top-down approach was utilized by harnessing the separation power of size exclusion chromatography (SEC), reversed phase liquid chromatography (RPLC) and CE.[19] This SEC-RPLC-CE-MS/MS multi-dimensional system was used to improve peak capacity as well as increase the sample loading volume from 200 nL to 1 μL. This was accomplished with a multi-dimensional approach as outlined in Figure 3. By subjecting each of the 5 fractions collected by size exclusion chromatography to further fractionation by RPLC, a total of 100 fractions were sorted prior to CE analysis of each fraction. The offline 3-dimensional separation had an estimated total peak capacity of 4000. Sample loading in the CE was increased with a pH-junction for sample stacking that was achieved by placing samples in pH 8 buffer and separating in pH 2 buffer. Compared to traditional techniques, this method enabled the identification of 10 times more proteoforms in the *E. coli* proteome. Over 5,700 proteoforms and 850 proteins were identified with a false-discovery rate of 1%. Post translational modifications (i.e. methylation, acetylation, etc.) were also identified with MS/MS analysis. The proteoform abundance was correlated to two different genes (hdeA and hdeB) under investigation. Most of the proteins in *E. Coli* did not contain post translational modifications. Moreover, the percentage of proteins involved with a specific function (i.e. cellular processes or catalytic activity) was comparable to data in the UniProt database. This multi-dimensional approach generated the largest reported top-down proteomics database at the time the report was published.[19]

This technique was also employed for analysis of *E. coli* proteins under native conditions.[20] Over 100 proteins and nearly 700 proteoforms with molecular weights below 30 kDa were identified. In this work, 23 protein complexes were identified, 14 of which have not previously been reported. The combination of strong cation exchange (SCX), RPLC and CE to form an SCX-RPLC-CE-MS/MS system was reported for a bottom-up approach to identify 8,200 proteins and 65,000 peptides in mouse brain.[21] Compared to 2D-LC-MS/MS alone, 10% more peptides and 40% more proteins could be identified. In other multi-dimensional proteomics research, nanoflow RPLC used prior to CE-MS/MS analysis increased the number of detectable proteins[22] With this RPLC-CE system 7500 proteins and almost 60,000 peptides were identified in only 5 μg of cells used to study breast cancer (MCF7). The detection of proteins with limited sample achieved with the system was attributed to reduced sample loss, good separation efficiency and sample concentration associated with the dynamic pH-junction.[19] The peptide mass was well correlated with the peak intensity ($R^2 = 0.98$) and the precision in protein identification below 10% relative standard deviation was achieved ($n = 3$).

The high separation efficiency of CE has also been leveraged for research on post translational modifications. CE-MS was demonstrated to be an effective technique to couple to traditional nanoLC-MS methods for identification and quantification of post-

translationally modified peptides. With CE-MS alone, over 5000 peptides were identified and over 4000 were quantified.[17] When compared to nanoLC, less than one third of the identifications overlapped, confirming the advantage of the combination of methods. Another strength realized with CE separations is the evaluation of microheterogeneity in glycosylation. The limits of detection reported in this area are below those obtained with traditional nano-LC methods.[23] With coupled RPLC-CE-MS/MS systems, analyses of mass-limited samples were achievable.[24] Glycoproteomic identification of samples of approximately 200 ng by CE-MS/MS surpassed that obtained with UPLC.[25] The higher throughput of CE-MS/MS required new algorithms to quickly process the large amounts of data.[26,27] These algorithms allowed for the identification of over 2.5 times more peaks, enabling the detection of 27,000 peptides and 4400 proteins in human cells.

The low volume sample requirements of CE are ideally suited for single-cell proteomics. Analysis of a single cell provides information about proteins and peptides that can be indicative of function or developmental stage. To demonstrate the feasibility of single-cell analysis with CE-MS, a single cell from a frog embryo (*Xenopus laevis*) was sampled at 4 points throughout development.[28] Samples were collected at the 16-, 32-, 64- and 128-cell stages. At each stage, a 10 nL volume of cellular fluid was removed from a single midline animal-dorsal (i.e. D11) cell. Sampling from the D11 cell was particularly relevant because this cell ultimately develops into neural tissue. Moreover, the location of this cell can be determined based on cell fate-mapping. Results from each stage of development were compared to the first sample collection of the D11 cell at the 16-cell stage. It was determined that of the 456 quantifiable proteins, 91 had statistically different concentrations from the measurements obtained at the 16-cell stage. Using 5 ng of digested protein collected with a custom microprobe, CE-MS identified 360 proteins per cell compared to 282 proteins/cell observed using whole-cell dissection. Because of the small sample volume available with single-cell analysis, low limits of detection are required. A detection limit of 700 zmol was estimated for this system using angiotensin peptide. The potential for this technique to be used with even smaller cells was demonstrated using 33 pg of protein digest from embryonic zebrafish (*Danio rerio*) cells. These cells are smaller in size in comparison to the *Xenopus laevis* discussed earlier. Samples were collected from 3 cells each from a different embryo in the 2-cell stage of development. Over 300 proteins were quantified. The peak intensities for the proteins in the zebrafish cells varied significantly across embryo, which was postulated to be a function of biological variability in the cells. Future work in targeted analyses was proposed as a method to elucidate the origin of the observed differences in cellular proteins.

1.3 Protein-based Therapeutics

Biopharmaceuticals, and in particular protein-based therapeutics,[29,30] comprise a growing market of a new class of drugs for healthcare innovation. The analysis of protein-based therapeutics is important to drug discovery, manufacturing and the evaluation of generics. There is a need to analyze protein charge variants, which can readily be accomplished using capillary isoelectric focusing. In this mode of CE, a pH gradient is generated in the separation capillary. With electric field superimposed across the capillary, sample molecules included within this pH media are positioned at the region where the molecule is neutral.

Once the pH focusing of ampholytes and analytes is complete the resolved peaks are imaged in capillary or are mobilized to the detector. Isoelectric focusing sorts proteins within the capillary according to the protein isoelectric point, which is the pH value at which the net protein charge is zero. This methodology is well suited to protein-based therapeutics because changes to the protein through degradation or other modification will impact the isoelectric point. The resolution of this technique depends upon the pH range selected by the user, the quality of the ampholyte gradient and operation of the method under conditions that minimize extra-column band broadening. This method is becoming more widely adopted for biological characterization and attention is directed to validation to support routine use of capillary isoelectric focusing. An interlaboratory validation of imaged capillary isoelectric focusing coupled with absorbance detection was performed using the criteria outlined by the International Council for Harmonization of Technical Requirements for Pharmaceuticals for Human Use.[31] Three monoclonal antibodies were utilized, which were IgG1 anti-VEGF, IgG2 anti-RANKL and IgG4 anti-PD1, by 10 different laboratories. With the precision of ± 0.01 pH units the method was suitable as an identity assay and for purity assessment. Beyond the use of imaged capillary isoelectric focusing for purity analysis, an emerging application of the method is the determination of positions in the protein that are susceptible to degradation.[32]

There is a concerted effort to increase the power of capillary isoelectric focusing by leveraging the structural information achievable with mass spectrometry. Capillary isoelectric focusing was interfaced with mass spectrometry[33] using a previously described flow-through microvial interface.[34] The approach is depicted in Figure 4 and involved separation with different commercially available ampholytes and a neutral capillary.[33] Following development of the separation method, a resolution of 0.02 pH units was achievable for peptides. Following the isoelectric focusing step, the protein bands were mobilized to the mass spectrometer through a combination of pressure-driven flow and electromigration by replacing the catholyte with acidic buffer that also contained methanol. The power of this technology was demonstrated with the chimeric monoclonal antibody infliximab, distinguishing the therapeutic antibody from 3 charge variants. Through the analysis of 33 ng of protein the variants with an Orbitrap Fusion Lumos mass spectrometer, it was established the variants resulted from clipping of c-terminal lysine (Figure 4, peaks K1, K2) or asparagine deamidation (Figure 4, peak D). In a separate report a method of CE mobilization was established to transfer the therapeutic monoclonal antibody herceptin to the mass analyzer.[35] The herceptin had been resolved from a small basic variant with imaged capillary isoelectric focusing.[35] With appropriate valving and electrophoresis the methyl cellulose and ampholyte additives used in the isoelectric focusing were eliminated from the spectra. Other reports of extensive characterization of antibody therapeutics have leveraged the versatility and effectiveness of CE-MS systems. A middle-up strategy involving cleavage of the antibody at the hinge region[36] utilized a similar, but commercially available interface[37] identifying the cause of charge heterogeneity for 11 charge variants of the therapeutic antibody cetuximab. In another report through the analysis of intact antibody the presence of dissociated light chain in the antibody preparation was observed.[38] Further middle-down analyses utilizing tandem MS of antibody cleaved at the hinge region identified differences in deamidation and glycosylation.[38]

Other modes of capillary electrophoresis are also utilized for the evaluation of biological therapeutics. This includes the use of capillary gel electrophoresis size-based sieving of proteins to rapidly screen for antibody impurities[39–41] and to investigate protein fragmentation.[41,42] A more selective Western blot capillary electrophoresis approach was reported to identify antibody fragmentation.[43] With this technique antibody fragments which had been separated with size exclusion chromatography prior to capillary electrophoresis were visualized with fluorescent probes specific for the kappa light chain, as well as the Fc and Fab regions of an IgG.

1.4 Enzyme Analyses

Immobilization of enzymes onto supports allows for the possibility to reuse the enzyme, which in turn lowers the cost associated with each experiment. Immobilized enzyme microreactors (IMERs) make it possible to perform an in-line enzymatic assay. There are three different strategies for immobilization: immobilization to a monolith created by polymers, immobilization onto membranes or particles which creates a packed IMER and immobilization onto the capillary surface, which creates an open tubular IMER. Monolithic enzyme microreactors can increase efficiency and throughput of sample preparation. Organic monoliths are advantageous due to good biocompatibility, pH stability, easy preparation and surface chemistry modification. An organic monolith was reported for proteolytic digestion using a trypsin based IMER.[44] Trypsin was immobilized to the monolith by covalent attachment to amines on the trypsin. The IMER was functional for a period of 25 days as evaluated by monitoring the area of product generated by incubation with the substrate *N*α-benzoyl-L-arginine ethyl ester. A 40 s column digestion of cytochrome c generated the same fragments obtained with overnight incubation with free trypsin in solution digestion. IMERs can also be fabricated by packing modified particles inside the capillary for immobilization support of enzymes. A packed IMER was described in which trypsin immobilized on cellulose resin was packed as a 7.5-cm reaction bed that was connected to a 64.5 cm separation capillary.[45] The packed reaction bed could be used for up to 10 reactions. When applied to CE-MS for bottom-up analysis of standard proteins or *E. coli* lysate digestion, separation and mass analysis was complete in under 30 minutes. A porous hydrogel IMER with a high loading capacity was simple to fabricate using alginate, which is a polysaccharide.[46] The capillary was loaded with a zone of alginate, enzyme and calcium carbonate. At lower pH, calcium ions are released from the calcium carbonate and the calcium cations cross-link the alginate matrix. The process is triggered by selecting an enzyme-substrate pair that will decrease the pH upon product formation. Both acetylcholinesterase[46] and penicillinase[47] were leveraged to mediate cross linking and subsequently encapsulated to form an IMER.

Permanently packed IMERs cannot be easily regenerated and must be replaced. Magnetic particles are held in place with a magnetic field superimposed on the capillary as shown in Figure 5. Magnetic reaction beds are an alternative to packed IMER beds, and offer the unique advantage of being easily replaced or exchanged by removing the magnetic field to expel the particles from the capillary through a simple rinsing procedure. Magnetic microparticles are available with different functional groups allowing for flexibility in the immobilization chemistry. The effect of the type of functional group on immobilization was

evaluated for sulfotransferase 1A1 to achieve maximum enzyme activity.[48] Studies like these help determine immobilization techniques best suited for different types of enzymes. Magnetic nanoparticles are also used for enzyme immobilization. For example, a polymer modified magnetic nanoparticle was used to obtain alanine aminotransferase kinetics using chiral ligand exchange capillary electrophoresis.[49] The enzyme reactor composed of polymer modified magnetic nanoparticles had improved stability over enzyme in free solution as the immobilized enzyme maintained 80% of its original activity after 5 weeks. Additional examples of modified magnetic microparticles have been employed, including poly(styrene-co-maleic anhydride-acrylic acid) modified particles.[50] To increase utility of the approach for commercial capillary electrophoresis systems, a 3D printed magnet holder was described.[51] Placement of the magnet was optimized as to not disrupt coolant flow and was compatible with either liquid or air based coolant systems (Figure 5).

Open-tubular IMERs are also employed with capillary electrophoresis because they can be fabricated using programmable rinsing with an automated instrument. One study utilized the exposed silica surface of the inner capillary wall for the immobilization of thrombin in order to evaluate the inhibitory effect of catechins.[52] Traditional open-tubular based IMERs can suffer from a smaller enzyme-substrate contact area than other IMERs. To overcome this, a method was developed to produce a porous-layer modified open-tubular IMER to increase the surface area and the enzyme loading.[53] To produce the porous layer, a biphasic sol-gel was used and enzyme immobilization was performed via ionic binding to a positively charged coating on the capillary surface. This resulted in improved enzyme activity compared to that obtained in free solution to 82% in the IMER after 7 days. After 10 cycles of inhibition and reactivation, the IMER retained 80% of its original enzyme activity.

Enzyme-substrate analyses in CE continue to offer high resolution and fast separations of limited sample volumes. On-line reactions reduce sample handling and thereby improve reproducibility and allow for automation. When the mobility of substrate and product are sufficiently different, capillary electrophoresis allows for the analysis of enzyme activity by monitoring product formation or depletion of substrate. The enzyme activity is defined by the Michaelis-Menten constant, K_m, which is the substrate concentration at half of the maximum velocity of the enzyme. A small K_m means maximum velocity is reached at low substrate concentration. Evaluation of K_m with on-line reactions is simpler and preferable to off-line reactions. In the period under review, K_m values were quantified on-line with CE-UV absorbance detection for a variety of enzymes including ecto-5-nucleotidase,[54] human recombinant matrix metalloproteinase,[55] human neutrophil elastase,[55] bovine testicular hyaluronidase,[55] histone deacetylase,[56] thrombin,[52] human nucleoside/nucleotide kinases.[57] In other reports K_m values were quantified on-line with CE-fluorescence detection for d-amino acid oxidase[58] and BCR-ABL.[59] Further, K_m values have been determined using on-line CE-UV detection for immobilized enzymes like penicillinase,[47] acetylcholinesterase,[46,53] alanine aminotransferase,[49] trypsin,[44] and β-glucosidase.[60] The values obtained on-line are comparable to off-line determinations. For example, on-line and off-line determinations of K_m values for penicillinase were 65 ± 7 μM and 73 ± 6 μM, respectively.[61] On-line evaluation of K_m with CE is also useful in comparing activities of enzymes, such as penicillinase and recombinant metallo-β-lactamase, two enzymes responsible for the deactivation of antibiotics, which had comparable K_m values.[61]

The identification of enzyme inhibitors is important in developing biotherapeutics. When inhibitors are present the enzyme activity is decreased. CE continues to offer fast identification of inhibitors. In one approach, 14 inhibitors for thrombin were identified using transverse diffusion of laminar flow profile-capillary electrophoresis (TDLFP-CE) in less than 2 minutes per run.[62] CE has been used to compare inhibitors of native and recombinant enzymes.[61] In the period under review, inhibitors of enzymes in free solution have been characterized with UV detection for ecto-5-nucleotidase,[54] thrombin,[52] histone deacetylase,[56] glucosamine-6 phosphate synthase,[63] human acetyl-CoA carboxylase 2,[64] and with laser induced fluorescence for d-amino acid oxidase[58] and BCR-ABL.[59] Further, inhibition studies have been done for immobilized enzymes including acetylcholinesterase[46,53] alanine aminotransferase,[49] beta-glucosidase,[60] and sulfotransferase 1A1[48] using UV detection.

Mixing during on-line incubation is advantageous over static enzyme reactions due to an observed increase in the rate of reaction.[52] In electrophoretic mediated micro analysis (EMMA) mixing is accomplished by colliding the enzyme and substrate zones. In this method, when the enzyme exhibits zero or very low electrophoretic mobility it is injected first, followed by the substrate, which has a higher electrophoretic mobility. Voltage[56] or voltage with polarity cycling[62] is then applied to drive the substrate through the enzyme zone. To improve conversion in EMMA analysis, the substrate is electrophoresed through the enzyme plug at a low voltage.[56] However, EMMA requires the enzyme to have sufficiently low electrophoretic mobility as compared to the substrate and the precise position of the enzyme plug must be known. Transverse diffusion of laminar flow profiles (TDLFP) has been used as an alternative method of mixing and does not require as much optimization as EMMA. In TDLFP, the enzyme and substrate plugs are hydrodynamically injected into the capillary, which generates a parabolic profile for each plug. This enables each plug to penetrate the previous plug injected and results in mixing. Applying reverse and forward pressure pulses further increases mixing in TDLFP. A recent report compared EMMA and TDFPL for inhibitory screening of thrombin using 4 inhibitors.[62] A lower percent inhibition was obtained with EMMA, which was attributed to inadequate mixing of the substrate and enzyme. When implemented properly, both TDLFP and EMMA provide rapid and streamlined measurements of enzyme activity and inhibition.

2. Pharmaceuticals

CE is a well-established technology in the field of small molecule drugs because of the efficiency, throughput and automation of the method. The application of CE for chiral resolution is substantial because of the low working solution volume required for separations (e.g. 3 mL total) and the flexibility to rapidly change the composition of background electrolyte. With CE it is unnecessary to immobilize the chiral selector in the separation capillary. Instead, a secondary equilibrium is superimposed in the electrophoresis to affect the migration of enantiomers. The preferential interaction of one enantiomer over another sorts the chiral molecules in a separation-based assay. In general, chiral selectors will display a difference in chiral recognition for enantiomers. In addition, additives such as cyclodextrins can distinguish molecules based on subtle differences in size through host:guest chemistry. Chiral CE separations require a thoughtful method design in order to ensure that molecular interactions favor the enantiomeric separation. For example, charged

enantiomers can be differentiated by mobility shifts arising from binding to neutral selectors. Conversely, neutral molecules must engage with charged selectors. The simplest separations are of a set of only 2 chiral compounds. However, it is desirable to develop methods that fully resolve a complex mixture of many chiral compounds in order to create a system applicable to a wide variety of pharmaceutical analyses. This process of method design is often empirical. Investigating incremental changes in different variables including the type of additive(s), concentration of additive(s) and pH are time consuming. Molecular docking software has been used to characterize host:guest binding and guide method development.[65–68] Recently, an approach to streamline the selection of an appropriate concentration of the chiral selector was described.[69] With preliminary information about the electrophoretic mobilities of the free and complexed molecular target as well as knowledge of the binding constants, the conditions leading to optimum resolution of the set are generated. Through other efforts, quality by design principles, which are widely described for pharmaceutical applications,[70,71] have been used in conjunction with multivariate analysis for the development of a chiral separation method.[72,73]

Cyclodextrins are cyclic sugar molecules with a cavity that enables enantioselective separations of chiral drugs. Beta-cyclodextrin[74–76] and β-cyclodextrin derivatives[65,73,77–84] are the most common additives used for chiral separations, although α-cyclodextrins[74] and γ-cyclodextrin derivatives[85,86] have also been reported. Cyclodextrins modified with different functional groups were used to resolve different drug enantiomers including methylated β-cyclodextrin for psychoactive drugs in under 4 minutes.[81] Another report synthesized 10 different methylated β-cyclodextrins to determine an optimized modification for chiral selection, which was found to be the heptakis (2,6-di-*O*-methyl)-β-cyclodextrin.[84] Sulfated β-cyclodextrins were used to determine enantiomeric impurities in the sedative dexmedetomidine.[73] Levels as low as 0.1% impurity could be detected. Beta-cyclodextrins have also been used in combination with other additives to facilitate chiral separations. This included combining β-cyclodextrin with acidic amino acids to improve the resolution of four basic drug molecules.[74] Enantioseparations were found to have 3- to 4-fold improvement in resolution with the use of deep eutectic solvents in combination with the cyclodextrins.[75] In one report the separation of multiple sets of chiral molecules was tailored to each enantiomeric pair by bracketing injected zones of enantiomers with different combinations of α-cyclodextrin, β-cyclodextrin, and maltodextrin.[87] In another application, β-cyclodextrins were combined with magnetic nanoparticles to enhance the detection of an antibiotic in blood and urine.[77]

Oftentimes, ionic liquids are used in combination with α-cyclodextrins,[88] β-cyclodextrins,[66,89] and γ-cyclodextrins,[90–92] to enhance selectivity. Ionic liquids are important to several techniques in the field of analytical chemistry.[93] These room temperature liquids, typically organic cations, are compatible with CE and are more frequently reported as an additive for chiral selection of pharmaceuticals. Another report successfully integrated ionic liquids with sample preconcentration achieved with field-amplified sample stacking.[89] This allowed for up to a 900-fold increase in the detection limit. The use of maltodextrin and dextrin in conjunction with ionic liquids has been reported to improve the resolution of drugs.[67,94] Chiral selectivity has been achieved by combining ionic liquids with non-dextrin additives.[68,95,96] One of these systems utilized tetrabutylammonium cations and chiral amino acid-

based anions to separate phenethylamines.[95] In the other example combining tetramethylammonium cations and clindamycin phosphate increased the resolution of 6 chiral drugs 2-fold better than was achieved in the absence of the ionic liquid.[68]

3. DNA Aptamers

DNA aptamers are single stranded oligonucleotide probes that can be generated to have high binding affinity for biomolecular targets. A method of aptamer selection based on systematic evolution of ligands by exponential enrichment, called SELEX, is used to generate aptamers from a combinatorial library that have binding affinity for a specific molecular target. Selection involves separating the non-binding sequences from the binding sequences and amplifying the binding sequences with polymerase chain reaction (PCR) amplification to create a new enriched pool of binding sequences. Repetitive rounds of positive selection for binding and negative selection to reduce non-specific binding are performed to evolve aptamer structure with the desired specificity and affinity. This process of selection is integrated with CE because oligonucleotide sequences bound to the molecular target undergo a mobility shift enabling separation and collection of high affinity aptamers. As an example, CE-SELEX was recently reported for the generation of an aptamer specific for the protein lactoferrin.[97] With CE-SELEX aptamers are generated in fewer rounds than that required with other techniques. However, the PCR amplification after each selection round in CE-SELEX is time consuming and can bias the aptamer pool. Non-equilibrium CE of equilibrium mixtures (NECEEM) alleviates these issues because PCR is not used in between enrichment cycles. A predictive tool for NECEEM was reported to estimate the number of selection rounds required to achieve enrichment of a DNA library for a targeted protein of a specified size and charge.[98] Recently, the NECEEM selection of a DNA aptamer for a biomarker of Alzheimer's disease was reported.[99] NECEEM has also been used to generate thrombin selective aptamers containing G-quadruplex structures, which are difficult to amplify with PCR.[100]

The process of selection and enrichment is simplified when the separation between non-binding and binding sequence is increased. A new technique called ideal filter capillary electrophoresis (IFCE) was introduced during the time frame of this review.[101,102] IFCE overcomes limitations of CE-SELEX and NECEEM because the target-binder complex and non-binding sequence migrate in opposite directions, which reduces the amount of non-binding sequences present in the fraction containing the binding sequences. This is achieved by adjusting the ionic strength of the running buffer to decrease the electroosmotic flow to be within a specific range. A consequence of this strategy is that the unbound oligonucleotide sequences are not detected. This confounds the calculation of the equilibrium constant (K_d) as well as the rate constant of complex dissociation (k_{off}). This shortcoming was mitigated by using pressure mobilization to drive the mixture past the detection window prior to initiating the electrophoresis separation of the bound and unbound oligonucleotide sequences.[103] With this method, termed double passage, the peak areas were obtained and K_d and k_{off} were determined. For IFCE, the position of the complex must be known in order to collect the bound oligonucleotides without contaminating the collected fraction with the unbound sequences. To circumvent issues that arise from detection of the complexed oligonucleotides, a mathematical model was described to predict the mobility of

the complex and thereby enable accurate collection of the complexed oligonucleotide sequences.[104] The advent of these advances in aptamer selection technology will streamline aptamer generation.

Once generated, aptamers provide molecular recognition in separation-based assays involving mobility shift of the bound and free target. Examples include the use of aptamers for monitoring pathogens in food samples. Detection of *E. coli* in milk and drinking water and their recovery were reported.[105] In a separate report a fluorescently labeled aptamer selective for the pathogen *S. Typhimurium*, was detected in spiked milk samples using a microfluidic electrophoresis fluorescence system.[106] In contrast to these reports of aptamer binding with large structures, the mobility shifts of aptamer binding with small molecules require a different separation strategy. A separation assay was designed in which mycotoxin binding to the aptamer displaced a complementary strand of DNA. The mycotoxin bound aptamer had a different mobility which could be distinguished from the mycotoxin-free aptamer.[107] In a different report, detection of Aflatoxin B1 was demonstrated using the duplex DNA formed by hybridization of cDNA with the aptamer.[108]

4. Metabolomics

Chromatography coupled to mass spectrometry is currently the gold standard for metabolomics work, but CE-MS is increasingly being utilized. CE-MS has been used to advance metabolomics research because of the potential for higher throughput analyses and suitability to separate small molecules with different charge-to-size ratios. Recently, a study was done with the goal of comparing the performance of CE-MS against LC-MS, through the analysis of plasma.[109] The study involved over 11,000 individuals in which 94 polar metabolites were identified. The results achieved with CE-MS were comparable to that of LC-MS. However, the CE method consumed less sample. These results strongly indicate that CE analyses will become more commonly used in metabolomics research. Metabolomics with CE-MS has recently been applied to give insight on the small biomolecules within tissues,[110–114] blood,[109,115–121] urine,[118,122,123] spinal fluid,[124] saliva,[125] and cells,[111,126–133] which can be used to improve health care associated with different types of cancer and other diseases. With the large quantities of data associated with metabolomics work, data processing software is paramount. Two types of novel processing software reported during this review period were ROMANCE,[116] which completed data analyses of a single peak in 2 minutes as well as Trace,[130] which reduced the total sample analysis time from weeks to hours. An additional noteworthy achievement was the development of a CE-MS database built upon the mobility of different metabolites to aid in rapid identification of analytes of interest.[131]

For most metabolomics work with CE-MS, the metabolites are analyzed in their native form with no derivatization. However, derivatization strategies for CE-MS analyses were described. One study reported the means to create a set of cationic metabolites as a result of derivatization with a tertiary amine.[134] This one-pot, two-step derivatization had the benefit of improving ionization efficiency of negatively charged analytes. In another publication, a method was developed to derivatize and resolve five D- and L-amino acids, as a strategy to detect D- amino acids in spinal fluid.[124]

Several other advances in metabolomics were realized during this review period. A unique approach to direct sampling of solid tissues by CE-MS was used to monitor metabolites without extraction or sample processing.[113] With this technology, the analyses were conducted with a variety of tissue samples from rat spinal cord, kidney and brain, revealing over 13,000 molecular features. High through put analyses of metabolites in dried blood spots offered rapid identification of cystic fibrosis in infants.[115] This multi-segmented injection-CE-MS system identified 32 new metabolites with analyses of seven multiplexed samples per run by performing alternating serial injections of background electrolyte and sample. In a different application, multi-segmented injection CE-MS was used for high throughput quantification of nonesterified fatty acids in serum samples.[135] Another improvement in metabolomics centered on the evaluation of analyses of small sample volumes. With an injection equivalent to a quarter of a cell (42 nL), one group identified 24 metabolites in a sample containing only 500 cells.[129]

Applications in single-cell metabolomics have emerged owing to the compatibility of CE-MS with small sample volumes. Single-cell omics provide information about heterogeneity, specific cellular function and changes in individual cells, which can be lost in traditional techniques that require cell averaging. Automated processing software supports this initiative,[130] and the effectiveness of this tool was demonstrated with the metabolomics data acquired from studying embryonic frog cells (*Xenopus laevis*).[128] The workflow for this process is summarized in Figure 6. To facilitate single cell sampling a 10 nL volume of embryonic cellular fluid was removed with a custom microprobe and efficiently extracted both anion and cations using a 4 μL volume of solvent. Two different separation conditions were established to resolve either the anionic or the cationic metabolites. Limits of detection for metabolites using this method were as low as 7.5 nM and 5.5 nM for cations and anions, respectively. With this method 4 cells were studied, each from a single embryo selected from different clutches. A total of 73 metabolites, comprised of 13 anionic, 49 cationic and 11 zwitterionic metabolites were identified and detected in the cells. Another research group conducting single cell metabolomics also employed a glass microprobe to facilitate the collection of less than 1 nL of cellular fluid from a single HeLa cell.[136] The sampling needle used in this work extracted less than 1 nL of fluid from individual HeLa cells. By preconcentrating the sample extracted from an individual cell using a combination of isotachophoresis and stacking,[137] 20 amino acids were quantified in the femtomole range, while 40 metabolites were identified in 4 cells.

5. Glycosylation

Carbohydrates are a fundamental class of biomolecules and play a critical role in energy, signaling, binding and communication. Protein glycosylation, which effects stability and function, is crucial for biological processes. Glycosylation is considered a biomarker of disease and impacts the efficacy of protein-based therapeutics. The detection and quantification of glycosylation is challenging because glycans are composed of monomers with only subtle structural differences. Moreover, saccharide monomers may be connected at different locations and orientations creating an array of isomers that must be detected. Protein glycosylation specific to asparagine residue (N-glycans) have a common structure containing a mannose core, but differ in the monomer composition as well as linkage. This

leads to structures with different levels of branching, including bisection. CE is used to identify and quantify glycosylation and is routinely accomplished with established chemistry that creates a 1:1 labeling specific to the reducing terminus of N-glycan structure. Free N-glycans are traditionally labeled with 8-aminopyrene-1,4,6-trisulfonic acid using reductive amination, although alternatives to this dye are commercially available.[138] The excitation maximum of these dyes matches the output of an argon ion laser. This enables detection of pico- to femtomole levels of N-glycans. In addition, this labeling strategy imparts a net negative charge that facilitates N-glycan migration in an electric field, rendering them easier to separate by CE. Though APTS labeling strategies for CE-laser induced fluorescence are well established, improvements upon reaction labeling continue to be reported. A report demonstrated that reactions subject to evaporation during labeling had higher product yield due to continuous concentration of reactants.[139] The study demonstrated that low reaction volumes improve the labeling efficiency but labeling efficiency could be further improved with the addition of tetrahydrofuran at the onset of the reaction. The extra tetrahydrofuran results in uniform sample uptake as a result of proper mixing allowed by the extra volume.

CE coupled with laser induced fluorescence provides a fast, automated approach for the analyses of N-glycans on protein therapeutics. Generic protein therapeutics, or biosimilars, must be compared to innovator therapeutics to demonstrate similar efficacy and structure. Capillary electrophoresis was used to validate that glycosylation of the biosimilar etanercept was in compliance with the innovator drug enbrel.[140] Differences in sialylation across manufacturers of recombinant human erythropoietin were demonstrated with CE.[141] The mannose content adversely impacts binding between antibody therapeutics, mannosylation of adalimumab was accurately quantified as a critical quality attribute in a wide concentration range.[142]

In addition to analyses of protein therapeutics, protein glycosylation is analyzed by capillary electrophoresis for health related applications. The N-glycans cleaved from transferrin were analyzed by capillary electrophoresis to evaluate congenital disorders of glycosylation.[143] In this study, CE was used as a preliminary approach to screen congenital disorders of glycosylation and identified decreased levels of sialylation when compared to controls. In a separate report, the cell-surface glycosylation on human induced pluripotent stem cell-derived cardiomyocytes was analyzed to assess cell viability for tissue transplant. Four parallel separation capillaries were employed in a commercial instrument with laser induced fluorescent detection to analyze the glycans cleaved from glycosphingolipids. With this approach 4 gangliosides (GM3, GD3, sialyl Lc 4 and nLc4) were reported as potential markers to distinguish pure stem cells from tumorigenic cells.[144]

Bisection of N-glycan structures is a potential biomarker of cancer. New methods have been developed to detect bisected N-glycans with CE-laser induced fluorescence. Capillary nanogel electrophoresis separations that utilize self-assembled phospholipid nanogels were used to resolve bisected N-glycans with different levels of galactosylation and sialylation.[145] This method achieved separation efficiencies of 500,000 theoretical plates with a detection limit of 70 picomolar when sample was electrokinetically injected. The thermal reversibility of the nanogel was leveraged to pattern stationary zones of lectin in-capillary. By integrating the lectin zone with nanogel separation the composition of the N-glycans was identified

without the use of standards or mass spectrometry. Nanoliter volumes of lectin were consumed in each run and the separation capillary was easily and repeatedly re-loaded with fresh lectin reagent for each separation using automated temperature control in a commercial instrument.

Sialic acid capping of N-glycans is related to several diseases, in particular the linkage between sialic acid and the penultimate galactose monomer is a potential biomarker of cancer. While it is critical to identify α2–3 vs α2–6 linked sialic acids, resolving these isomers in CE is challenging. Sialic acids are labile and are structurally difficult to distinguish. In one approach, the separation of sialic acid isomers was achieved following derivatization of the sialic acid moieties and analysis using microfluidic CE laser induced fluorescence.[146] As shown in Figure 7, a total of 17 different glycans were separated and detected as single peaks in less than 3 minutes. The carboxylic acids on sialic acids were neutralized by converting them to methyl amines. Resolution was achieved due to subtle differences in the hydrodynamic radius of different glycans containing α2–3 vs α2–6 linked sialic acids. Microfluidic electrophoresis-laser induced fluorescence enabled quantification of the structures that contained each type of sialic acid linkage. To correctly assign the structures for microfluidic CE-laser induced fluorescence, other complementary techniques were used, including CE-MS, LC-MS and MALDI-MS. Sialic acid linkage-specific alkylamidation, termed SALSA in many literature reports, was used to identify linkage according to the mass shift of α2–6 linked sialic acids (+41.063 Da) as compared to α2–3-linked sialic acids (+13.032 Da). Further, structural assignments were independently confirmed by cleaving the N-glycan mixture with a linkage specific enzyme, α2–3 sialidase and analysis of the cleaved N-glycan products.

A strategy to distinguish sialic acid linkage using derivatization chemistry and CE-MS was also reported.[147] For this research, free N-glycans were end-labeled using a cationic moiety to facilitate electrophoretic separation and improve electrospray ionization (ESI) in positive mode. The results are shown in Figure 8 where the extracted ion electropherograms are displayed according to abundance. The upper trace is of peaks at high abundance (> 2%). The middle trace is of N-glycans at intermediate abundance (from 0.5% to 1%). The lower trace is of N-glycans at low abundance (< 0.25%). Differentiation of the α2–3 vs α2–6 linked sialic acid isomers was achieved through a two-step derivatization process that resulted in ethyl esterification of α2–6 linked sialic acid (+319 Da) and amidation of α2–3 sialic acids (+290 Da). The CE-MS separation conditions were modified to be compatible with the MS analyses with a commercial CE instrument. Although these N-glycans were not fully resolved by the CE, the N-glycans within peaks were distinguished by the MS. In addition, structures of even low abundant peaks were identified. The separations obtained with the commercial instrument were longer than those reported with the microfluidic device; however, the CE-MS method did not need complementary techniques for structural identification.

Approaches to leverage both the separation efficiency of CE and structural identification of MS have also been described. CE separations of N-glycans were further analyzed using drift tube ion mobility-MS.[148] This approach identified isomeric α2–3 vs α2–6 sialic acid linkages due to differences in drift time. CE-MS analysis of the distribution of all N-glycan

features was reported for different therapeutic antibodies.[149] This middle-up approach involving cleavage at the antibody hinge region identified 32 charge variants in the Fc region, including sialylation. In a further effort to expand the use of CE-MS for structural analyses of glycoprotein therapeutics, a validated method was reported to characterize and quantify glycosylation of 10 monoclonal antibodies.[150] Glycopeptides from each antibody were analyzed both with CE-ESI-MS and HILIC separations, producing similar results as established through a comparison of the abundance of different N-glycan structures.

Quantification of N-glycans in mass spectrometry can be impacted by differences in ionization efficiencies. Instrumental modifications have been reported to address this by simultaneously using laser induced fluorescence detection with CE-ESI-MS. Laser induced fluorescence was used to quantify glycans within the ESI Taylor cone obtained with a commercially sourced porous sheathless tip.[151] Peak areas of N-glycans had intra- and inter-day reproducibility of 4% and 7%, respectively when measured with laser induced fluorescence. In order to compare the laser induced fluorescence response to the mass spectrometry signal, the percent area obtained for each N-glycan peak relative to the total N-glycan area was determined using both detectors. The percent area distribution obtained with MS revealed a significant decrease in signal for slower migrating peaks in comparison to the peak areas obtained with laser induced fluorescence. An alternative approach to N-glycan quantification with laser induced fluorescence prior to mass analysis adapted the cartridge of a commercial capillary instrument[138] to interface the capillary with a commercial microvial ESI source.[37] The capillary was configured outside of the commercial CE instrument by extending the length to 45 cm, making it possible to insert the capillary outlet into the ion source using sheath flow.[138]

Heparins are complex glycosaminoglycans consisting of repeating units of disaccharides, comprised of N-acetyl glucosamine linked to a hexuronic acid sugar. The N-acetyl glucosamine can be deacetylated or sulfated, while the hexuronic moiety is either glucuronic or iduronic acid. CE separations of heparins are performed in reverse polarity because heparins are highly anionic. They impact several biological processes through protein interaction, driving the characterization of the heparin structures in relation to these interactions. In one report, CE-MS operated with negative mode electrospray ionization was used in the analysis of heparin/heparin sulfate with up to 12 repeat units.[152] Separations were achieved with an acidic background electrolyte and a cationic coating, which generated a strong electroosmotic flow toward the detector. In a separate CE-MS approach, gas-phase sequencing of heparin was accomplished by using negative electron transfer dissociation.[153] Unlike collision-induced dissociation, fragmentation with negative electron transfer dissociation was achieved without sulfate decomposition. Structural and chemical information was obtained for the anticoagulant heparin drug, enoxaparin, which contained a mixture of low molecular weight heparins as well as isomeric structures. In a different report, capillary isoelectric focusing was used to separate mixtures of heparan sulfate and chondroitin sulfate.[154] Glycosaminoglycans were focused under reverse polarity according to subtle differences in isoelectric point, which was related to the level of sulfation in different structures.

6. Instrumental Advances

6.1 Microfluidic Free Flow Electrophoresis

Microfluidic free flow electrophoresis (FFE) is a tool enabling continuous throughput separations that uses a wide channel in which electric field is delivered perpendicular to fluid flow. Some practical limitations of this method, including stream broadening, bubble formation and joule heating, were investigated to expand the applicability of the technique. Increased resolution with FFE was reported through spatial confinement of the injected sample to avoid the walls of the separation chamber using spatially restricted injection and collection zones.[155] In a separate report, stream broadening was reduced by increasing the flow rate ratio of buffer to that of the sample.[156] Reduced sample loading was a consequence of both approaches.[155,156] To address bubble formation at the electrodes due to electrolysis in the anodic and cathodic reservoirs, a design was reported that positioned electrodes downstream of a fluid counter flow that isolated bubbles from the electric field driving the separation.[157] Finally, an analytical theory was presented in order to quantify the effect of joule heating on stream width and drift of analyte from the equilibrium position.[158]

Several advances in FFE were reported during the time frame of this review. A theoretical framework was introduced to enhance the optimization of FFE.[159] Analyte streams in FFE were modeled in terms of deflection angle (i.e. angulagrams) and the prevalent factors that dictated molecular stream resolution were identified (i.e. stream width, linearity and deflection). This proposed approach to characterize separation performance in FFE was created as a tool to evaluate fundamental parameters that guide FFE method development towards achieving a targeted molecular stream resolution. Through other efforts, FFE was adapted to selectively isolate target proteins and antibody biomarkers from a complex mixture using ssDNA probes.[160] Off chip signal amplification of the isolated protein was performed using catalyzed hairpin assemblies. In a different report, ampholyte free pH gradient generation was developed for a free flow isoelectric focusing system using concentrated acidic and basic solutions.[161] This approach was used to recover the proteins in fresh egg white and successfully separated ovomucoid in the pH 4.1 region, ovalbumin in the pH 4.5 region and ovotransferrin in the pH 6.3 region.[161] Moreover, FFE has been integrated with gradient generation to realize simultaneous analyte separation and concentration and has the potential to tailor separations of biomolecules.[162] Beyond protein analyses, the flow through nature of this technique is well suited for chemical reactions,[163–165] which is a fundamental step towards realizing emerging biomolecular applications such as on-demand drug synthesis.

6.2 Detection and Detector Interfaces

Instrumental advances include modification to common CE-MS interfaces based on sheath flow or sheathless electrospray designs. For instance, a new interface was fabricated that enabled switching between nano-sheath or porous frit operation by replacing the nano-flow sheath liquid with conductive liquid and positioning the capillary to protrude beyond the conductive liquid capillary.[166] When directly compared to a traditional triple tube interface, up to 87-fold increase in intensity was observed for monoclonal antibody. A thin wall tapered tip interface, which is conceptually similar to a porous tip, generated a 3.5-fold

increase in signal intensity relative to commercial porous tips.[136] The benefit of this design was the ability to use a 5 μm i.d. capillary which was compatible with low fluid flow rates that precluded the need for pressure-driven flow.

Instrumental modifications are also described. A lab-built capillary electrophoresis instrument in which both capacitively coupled contactless conductivity detection (C^4D) as well as mass spectrometry were integrated was designed to perform separations utilizing non-aqueous CE.[167] The power of the dual detection system was demonstrated with a food supplement where inorganic ions were detected with the C^4D and organic ions were detected with the MS. An adaptation to the standard capillary diameter accepted for commercial instruments was devised through the use of fused silica sleeves around the detection window and electrode assembly.[168] The use of the 30 μm inner diameter and 150 μm outer diameter capillary enabled the simultaneous detection with UV and MS detection. Strategies for better electrical decoupling to commercial instruments have been described.[169] Additionally, a simplified approach for self-alignment of the separation capillary and MS was developed through laser machining of polyimide and was compatible with a variety of capillary sizes as well as a commercial CE instrument.[170]

Investigation of optimization of electrical decoupling of CE and MS interfaces is continuing. In one study it was reported that decoupling the electrophoresis and electrospray voltage was more effective with the nano-sheath interface as compared to a sheathless porous tip.[171] Improved decoupling through the use of the separation capillaries with cracks resealed using dialysis membrane allowed for the detection of 52 cellular metabolites, reported to be twice the number observed with traditional sheath flow CE-MS.[172] In a different strategy, microchip electrophoresis was coupled to ESI-MS through the use of a hydrogel membrane at the base of the Y-junction in the microchip, decoupling current while directing sample to the mass spectrometer.[173]

A novel application with a newly developed CE-MS technique was demonstrated in determining protein structure through hydrogen-deuterium exchange (HDX).[174] As opposed to other methods that use CE to separate different isomers prior to HDX in the MS or MS interface, the method described completes the HDX in-capillary prior to MS analysis. A surface coating was employed to suppress the electroosmotic flow which facilitated analyte separations based primarily on electrophoretic mobility. In this technique, deuterated buffers were used as the background electrolyte. As a result, isomers with slower mobilities spent more time in the capillary and experienced higher levels of deuteration. This was detected with a mass shift in the corresponding mass spectra, providing insight into the accessibility for hydrogen and deuterium exchange. This approach was demonstrated with both myoglobin and lysozyme. Results obtained with this method were in agreement with structural analyses reported in the literature with X-ray crystallography. Deuterium exchange was less prominent in helical regions of the proteins owing to the stability and structure in these regions.

7. Future Directions

7.1 Single-cell Analyses

While impressive analyses of metabolomics in individual cells have been demonstrated,[128] strategies for targeted analysis of metabolites in single cells continue to leverage CE. A microfluidic device was reported for the measurement of glutathione in single liver cells using CE. Chemiluminescent detection sensitive to thiols was achieved using post-column reaction with hydrogen peroxide and luminal. Separations accomplished in under 2 minutes were used to analyze 10 individual cells.[175] In another report formaldehyde was detected in single cells using a commercial capillary electrophoresis instrument equipped with laser induced fluorescence detection.[176] HeLa cells were incubated with propyl-4-hydrazino-naphthalimide which readily reacted with formic acid. An individual cell was then manually aspirated into a capillary housed in a commercial cartridge with the aid of an optical microscope.

Single cell analyses are also performed to estimate enzyme activity using intracellular reporters. When these fluorescent substrates are introduced into single cells they are cleaved by cellular enzymes. Determining the enzymatic products in an individual cell provides rich information about enzyme function. In one report, the effectiveness of three methods of loading were performed to evaluate the performance of pinocytosis, electroporation and myristoylation. Cells lysed and analyzed via CE demonstrated significant differences in enzymatic processing across these loading methods. This was attributed to differences in the localization of the peptide reporter in the cell.[177] In a different report the activity of sphingosine kinase was evaluated in individual U-937 cells, K-562 cells and in primary cells from patients with chronic lymphoblast leukemia. A chemical fixation step was used to arrest the cellular metabolism and more effectively capture the chemical profile of sphingosine. The approach involved loading sphingosine-fluorescein into the cells and allowing the sphingosine-fluorescein to be converted to different metabolites. Following incubation, the cells were treated with the aldehyde fixative glyoxal. Fixed cells were loaded into the separation capillary with a pulsed laser. Lipids were extracted in-capillary, separated within 500 seconds and the fluorescent sphingosine metabolites were quantified. With this technique, a significant difference in kinase metabolism was observed when cells were treated with inhibitors.[178]

CE methods enabled analyses of multiple proteins in a limited number of single cells,[28,136] but also facilitated the targeted detection of a particular protein in a large population of cells. An important advantage of microfluidic electrophoresis is the capacity for high throughput analysis by patterning many channels on one device. Such strategies result in rapid and simultaneous separations. To realize high throughput screening in single-cell polyacrylamide gel electrophoresis (PAGE), an open microfluidic device was reported with hundreds to thousands of coated microwells patterned on a polyacrylamide coated glass slide.[179] Applying this design, interactions of epithelial cellular adhesion molecule (EpCAM) and MCF-7 breast cancer cells were investigated using single-cell microchip immunoblot and single-cell PAGE.[180] Cells were lysed and proteins were injected into the gel and separated. Following the separation, the proteins were immobilized to the gel matrix. Detection was

then achieved with fluorescent antibody probes. To determine whether the proposed platform is on par with current techniques used to measure surface receptors (i.e. flow cytometry and immunofluorescence), the fluorescence intensity from the anti-EpCAM stained cells was analyzed via flow cytometry and immunofluorescence. These methods of single-cell PAGE, flow cytometry and immunofluorescence produced similar fluorescence intensity profiles, demonstrating that microfluidic single-cell PAGE is an acceptable alternative to traditional techniques used to accurately measures surface bound receptors.

Microfluidic devices also offer a means to model in vivo environments and investigate cell-cell interactions. For example, a body-on-chip microfluidic device integrated with CE, was used to shed light on the role of adipocytes on insulin levels produced by islets of Langerhans.[181] In response to high glucose levels, β-cells in islets secrete insulin. The process of insulin release was observed to oscillate. Nonesterified fatty acid esters produced by adipocytes modulated insulin. To shed light on this process a solution was passed through a chamber in the microfluidic device harboring adipocyte cells in order to collect and transfer nonesterified fatty acid esters to the islet. The buffer in the adipocyte chamber was then perfused over the islet chamber in the microfluidic device for 3 hours. This liquid transfer was facilitated by the microfluidic device design in Figure 9. Glucose solutions were then passed over the islet and stimulated insulin secretion was measured using an electrophoretic immunoassay. The electrophoretic assay was performed by continuous sampling from the reservoir holding the islet. The sample was mixed with fluorescently labeled insulin as well as antibody in the reaction channel and transferred every 8 seconds to the separation capillary where the bound and free insulin peaks were quantified. Insulin sampling at 8-second intervals was maintained for 30 minutes. This fast readout time provided good temporal resolution. A more substantial release of insulin from the islet of Langerhan was observed following exposure to the adipocyte perfusate as compared to exposure to equivalent levels of nonesterified fatty acid standards. This finding indicated that other factors released by adipocytes also potentiated insulin release. With this enabling technology, the body-on-chip device provided the means to elucidate these additional factors.

7.2 Separations of Biological Particles

Recently, extracellular vesicles known as exosomes, have become a topic of interest as exosomes contain proteins, RNA and DNA. Cells secrete and uptake exosomes in almost all types of bodily fluids, making them a noninvasive biomarker. A microfluidic electrophoresis device was designed to separate and concentrate exosomes by electrophoresis and an ion-selective membrane by continuously trapping exosomes in agarose gel.[182] The device contained a delivery channel that intersected an exosome capture channel with two different methods of exosome selection. Plasma or serum samples were pushed through the delivery channel with pressure. Exosomes were preferentially driven into the capture channel with a superimposed electric field. In the capture channel exosomes passed through a porous agarose gel which excluded cellular debris that co-migrated with the exosomes. Exosomes were then electrostatically concentrated at a negatively charged cationic exchange membrane anchored at the terminus of the capture channel. High electric field produced high throughput capture of exosomes. Continuous flow from the pump prevented device clogging

by washing away debris. The device design minimized the formation of bubbles in the main channel and pH gradients resulting from electrolysis at the cathodic reservoir were mitigated by replenishing the buffer reservoirs frequently. This platform recovered 77% of the exosomes spiked in approximately 1 mL of blood or serum in 20-minutes, which was an improvement over commercial capture strategies that recovered 25% of the exosomes and required longer time for processing.

New advances in gene therapies and vaccines have created a need for analytical technologies capable of characterizing virus particles as well as nanoparticles used for drug delivery. A validated CE method was reported to rapidly and reproducibly quantify adenovirus in a vaccine.[183] Parameters were evaluated which were relevant to transferring the method to the facility tasked with in-process control testing of adenovirus content in a vector-based vaccine product. Adenovirus particles, which have a negatively charged surface,[184] were separated under reverse polarity in a 3-minute run with an automated instrument and a commercially available neutral coated capillary. Sample analysis was complete in 2 hours with CE. This was a significant improvement over the current method of choice, quantitative PCR, which required a minimum of a single day per sample. In a separate report, imaged capillary isoelectric focusing of mRNA lipid nanoparticle vaccines was developed as a tool to meet FDA recommendations for characterization and stability assessment.[185] Lipid nanoparticles serving as a delivery vehicle for mRNA were self-assembled from 4 classes of lipids: cationic lipids, zwitterionic lipids, uncharged lipids and polyethylene glycol lipids, with different lipid components serving a different purpose (i.e. cytosolic delivery, modulate fluidity, increasing circulating half-life). Separation of the nanoparticle achieved with a fluorocarbon coated capillary enabled characterization and quantification with absorbance detection. Different cationic lipid formulations were distinguished by differences in isoelectric points (e.g. ~7.65 vs 8.1) with capillary isoelectric focusing. Moreover, stability of the nanoparticle aggregate was observed as peak splitting following exposure to elevated temperature.

7.3 3D Printing of Separation Platforms

Glass and PDMS based microchips are common materials for microfluidic electrophoresis. However, the versatility and on-demand production of 3D printing have spawned efforts to leverage this technology for microfluidics. A single step automated printing of a sample-in/answer-out device in 40 minutes was reported using a 5-head fused deposition modeling printer.[186] Channels printed on this device had a width and depth of 800 and 500 μm, respectively. Different materials enabled integrated fabrication of several other key modules required for a point-of-care device, including an optically transparent detector cell, electrodes to drive the separation and membranes to exclude particulate and to concentrate the analytes. The device required no further sample handling once the background electrolyte and urine were loaded. Following extraction and concentration ampicillin was quantified within 3 minutes in untreated urine.

A barrier to fully realizing the advantages of 3D printing is difficulty in creating dimensions on the scale of capillary electrophoresis channels, which range from 10 to 75 μm in diameter. Methodology to enable stereolithographic 3D printing in this size regime was

developed[187] and further enhanced to fabricate microfluidic electrophoresis channels with 50 μm channels.[188] The device was fabricated to contain a T-shaped separation channel shown in Figure 10A. The channels, emphasized in Figure 10B, had a width and depth of 40 and 50 μm, respectively. These narrow channels were fabricated by blending a UV absorbing compound (i.e. 2% 2-nitrodiphenylsulfide) with the resin composed of (1% Irgacure in polymethylene glycol diacrylate). The UV absorber was compatible with the 385 nm LED in the digital light processor stereolithographic 3D printer and served to control the depth of optical penetration in the resin. The thickness of the layer was achieved by optimization of exposure, enabling reproducible fabrication of microfluidic devices with defined geometry. The performance of the 3D printed device was compared to devices with similar geometry that were fabricated from standard microfluidic materials. As evaluated through measurements of preterm birth markers, similar or marginally lower separation performance was reported with the 3D printed device in comparison to the devices made from poly(methyl methacrylate), polydimethylsiloxane, or cyclic olefin copolymer. This example of a portable means to measure molecules relevant to human health demonstrates the utility of CE to positively impact society. Growing use of new and exciting technologies to fabricate integrated devices for CE will render the method even more widespread and accessible.

ACKNOWLEDGMENTS

Research reported in this publication was supported in part by the National Institute Of General Medical Sciences of the National Institutes of Health under Awards Number R01GM114330 and P41GM128577. The content is solely the responsibility of the authors and does not necessarily represent the official views of the National Institutes of Health.

Biography

Courtney J. Kristoff is a Ph.D. candidate at West Virginia University. She earned her B.S. degree in chemistry from Waynesburg University in 2018. Her research involves capillary coatings and protein analyses using novel interfaces for coupling capillary electrophoresis and mass spectrometry.

Lloyd Bwanali received a B.S. degree in chemistry from National University of Science and Technology, Bulawayo, Zimbabwe. Lloyd is a Ph.D. candidate in chemistry at West Virginia University in Prof. Lisa A. Holland’s group. His graduate research work is focused on characterizing glycosylation establishing the impact of glycan post-translational modification on antibody efficacy.

Lindsay Veltri is a Ph.D. candidate at West Virginia University. She earned her B.S. in chemistry from West Virginia University in 2018. She is the recipient of the 2017 ACS Division of Analytical Chemistry Undergraduate Award and the College Chemistry Award from the Society for Analytical Chemists of Pittsburgh. Her academic interests include the design and application of microfluidic devices for medical diagnostics, carbohydrate research, cellular analyses, and the development of nanomaterials for biological detection.

Gayatri P. Gautam received his B. Sc. and M. Sc. degrees in chemistry from Tribhuvan University, Nepal and joined Prof. Menake E. Piyasena’s research group at New Mexico

Institute of Mining and Technology in 2014 for graduate studies. In his graduate studies, he worked on research projects related to microfabrication and separation of cells and particles in microfluidic platforms using acoustic forces. After graduation with his Ph. D. degree in chemistry, he joined Prof. Lisa A. Holland's research group at West Virginia University as a postdoctoral research fellow. His research interests include separations of biologically relevant small molecules using microchip electrophoresis.

Patrick Rutto graduated with a B.S. degree in chemistry from University of Eastern Africa, Baratom in 2016 and with a M.S degree in chemistry at Youngstown State University in 2018. He is enrolled in the West Virginia University PhD program in chemistry. As a member of Dr. Holland's research group, he focuses on the characterization of N-glycans using CE and CE-MS.

Ebenezer Newton graduated with a B.S. degree in chemistry from University of Cape Coast in 2009 and with a M.S. degree in chemistry from Rowan University in 2018. He joined the Ph.D. program in chemistry at West Virginia University and is a member of Prof Lisa A. Holland's research group. Ebenezer's graduate research centers on the development of CE based techniques for glycan analysis.

Lisa Holland is a Professor of Chemistry at West Virginia University, specializing in microscale separations of biomolecules relevant to human health. She received her B.S. degree in chemistry from the University of Maryland at College Park. She received her Ph.D. in chemistry from the University of North Carolina at Chapel Hill under the direction of Professor James Jorgenson. Through a National Research Service Award, she held a postdoctoral fellowship under the direction of Professor Susan Lunte in the Department of Pharmaceutical Chemistry at the University of Kansas. Dr. Holland is the recipient of a National Science Foundation Faculty Early Career Development award and has served as the Chair of the American Chemical Society Subdivision of Chromatography and Separation Chemistry. She enjoys teaching instrumental analysis to undergraduate and graduate students and mentoring the many outstanding researchers who have engaged in science at WVU.

References

(1). Mora MF; Jones SM; Creamer J; Willis PA Electrophoresis 2018, 39, 620–625. [PubMed: 29136289]

(2). Ferreira Santos MS; Cordeiro TG; Noell AC; Garcia CD; Mora MF Electrophoresis 2018, 39, 2890–2897. [PubMed: 30086207]

(3). Creamer JS; Mora MF; Willis PA Electrophoresis 2018, 39, 2864–2871. [PubMed: 30216482]

(4). Creamer JS; Mora MF; Noell AC; Willis PA Electrophoresis 2019, Early View 10.1002/elps.201900268.

(5). McCord BR; Gauthier Q; Cho S; Roig MN; Gibson-Daw GC; Young B; Taglia F; Zapico SC; Mariot RF; Lee SB; Duncan G Anal. Chem 2019, 91, 673–688. [PubMed: 30485738]

(6). Yu F; Zhao Q; Zhang D; Yuan Z; Wang H Anal. Chem 2019, 91, 372–387. [PubMed: 30392351]

(7). Ragland TS; Gossage MD; Furtaw MD; Anderson JP; Steffens DL; Wirth MJ Electrophoresis 2019, 40, 817–823. [PubMed: 30556148]

(8). Ouimet CM; D'Amico CI; Kennedy RT Anal. Bioanal. Chem 2019, 411, 6155–6163. [PubMed: 31300857]

(9). Kahle J; Maul KJ; Wätzig H Electrophoresis 2018, 39, 311–325. [PubMed: 28949023]
(10). Zhu Y; Li Z; Wang P; Shen L; Zhang D; Yamaguchi YJ Chromatogr. B 2018, 1083, 63–67.
(11). Morani M; Taverna M; Mai TD Electrophoresis 2019, 40, 2618–2624. [PubMed: 31116449]
(12). Yu B; Peng Q; Usman M; Ahmed A; Chen Y; Chen X; Wang Y; Shen Y; Cong HJ Chromatogr. A 2019, 1593, 174–182.
(13). Liu R; Cheddah S; Liu S; Liu Y; Wang Y; Yan C Anal. Chim. Acta 2019, 1048, 204–211. [PubMed: 30598151]
(14). Crihfield CL; Kristoff CJ; Veltri LM; Penny WM; Holland LAJ Chromatogr. A 2019, Epub ahead of print 10.1016/j.chroma.2019.460397.
(15). Leclercq L; Morvan M; Koch J; Neusüß C; Cottet H Anal. Chim. Acta 2019, 1057, 152–161. [PubMed: 30832914]
(16). Alharthi S; El Rassi Z Talanta 2019, 192, 545–552. [PubMed: 30348428]
(17). Faserl K; Sarg B; Gruber P; Lindner HH Electrophoresis 2018, 39, 1208–1215. [PubMed: 29389038]
(18). Geng Z; Song Q; Yu B; Cong H Talanta 2018, 188, 493–498. [PubMed: 30029403]
(19). McCool EN; Lubeckyj RA; Shen X; Chen D; Kou Q; Liu X; Sun L Anal. Chem 2018, 90, 5529–5533. [PubMed: 29620868]
(20). Shen X; Kou Q; Guo R; Yang Z; Chen D; Liu X; Hong H; Sun L Anal. Chem 2018, 90, 10095–10099. [PubMed: 30085653]
(21). Chen D; Shen X; Sun L Anal. Chim. Acta 2018, 1012, 1–9. [PubMed: 29475469]
(22). Yang Z; Shen X; Chen D; Sun L Anal. Chem 2018, 90, 10479–10486. [PubMed: 30102516]
(23). Qu Y; Sun L; Zhu G; Zhang Z; Peuchen EH; Dovichi NJ Talanta 2018, 179, 22–27. [PubMed: 29310225]
(24). Qu Y; Sun L; Zhang Z; Dovichi NJ Anal. Chem 2018, 90, 1223–1233. [PubMed: 29231704]
(25). Zhang Z; Dovichi NJ Anal. Chim. Acta 2018, 1001, 93–99. [PubMed: 29291811]
(26). Zhang Z; Hebert AS; Westphall MS; Qu Y; Coon JJ; Dovichi NJ Anal. Chem 2018, 90, 12090–12093. [PubMed: 30179504]
(27). Zhang Z; Hebert AS; Westphall MS; Coon JJ; Dovichi NJ J. Proteome Res 2019, 18, 3166–3173. [PubMed: 31180221]
(28). Lombard-Banek C; Moody SA; Manzini MC; Nemes P Anal. Chem 2019, 91, 4797–4805. [PubMed: 30827088]
(29). Kaplon H; Reichert JM mAbs 2019, 11, 219–238. [PubMed: 30516432]
(30). Agbogbo FK; Ecker DM; Farrand A; Han K; Khoury A; Martin A; McCool J; Rasche U; Rau TD; Schmidt D; Sha M; Treuheit NJ Ind. Microbiol. Biotechnol 2019, 46, 1297–1311.
(31). Wu G; Yu C; Wang W; Wang L Electrophoresis 2018, 39, 2091–2098. [PubMed: 29797663]
(32). King C; Patel R; Ponniah G; Nowak C; Neill A; Gu Z; Liu HJ Chromatogr. B 2018, 1085, 96–103.
(33). Wang L; Bo T; Zhang Z; Wang G; Tong W; Da Yong Chen D Anal. Chem 2018, 90, 9495–9503. [PubMed: 29993237]
(34). Zhong X; Maxwell EJ; Chen DDY Anal. Chem 2011, 83, 4916–4923. [PubMed: 21528898]
(35). Montealegre C; Neusüß C Electrophoresis 2018, 39, 1151–1154. [PubMed: 29469203]
(36). Dai J; Zhang Y Anal. Chem 2018, 90, 14527–14534. [PubMed: 30451489]
(37). Peuchen EH; Zhu G; Sun L; Dovichi NJ Anal. Bioanal. Chem 2017, 409, 1789–1795. [PubMed: 27981343]
(38). Belov AM; Zang L; Sebastiano R; Santos MR; Bush DR; Karger BL; Ivanov AR Electrophoresis 2018, 39, 2069–2082. [PubMed: 29749064]
(39). Gu Y; Voronov S; Ding J; Mussa N; Li ZJ Anal. Bioanal. Chem 2019, 411, 2425–2437. [PubMed: 30880351]
(40). Beckman J; Song Y; Gu Y; Voronov S; Chennamsetty N; Krystek S; Mussa N; Li ZJ Anal. Chem 2018, 90, 2542–2547. [PubMed: 29357216]
(41). Duhamel L; Gu Y; Barnett G; Tao Y; Voronov S; Ding J; Mussa N; Li ZJ Anal. Bioanal. Chem 2019, 411, 5617–5629. [PubMed: 31214752]

(42). Yang B; Li W; Zhao H; Wang A; Lei Y; Xie Q; Xiong SJ Chromatogr. B 2019, 1112, 1–10.
(43). Zhu Y; Ahluwalia D; Chen Y; Belakavadi M; Katiyar A; Das TK Electrophoresis 2019, 40, 2888–2898. [PubMed: 31271455]
(44). Cheng M; Wang R; Zhang B; Mao Z; Chen ZJ Pharm. Biomed. Anal 2019, 165, 129–134.
(45). Villegas L; Pero-Gascon R; Benavente F; Barbosa J; Sanz-Nebot V Talanta 2019, 199, 116–123. [PubMed: 30952234]
(46). Yang J; Hu X; Xu J; Liu X; Yang L Anal. Chem 2018, 90, 4071–4078. [PubMed: 29469571]
(47). Hu X; Yang J; Chen C; Khan H; Guo Y; Yang L Talanta 2018, 189, 377–382. [PubMed: 30086934]
(48). Ramana P; Adams E; Augustijns P; Van Schepdael A Electrophoresis 2019, 40, 2271–2276. [PubMed: 30882918]
(49). Feng W; Qiao J; Jiang J; Sun B; Li Z; Qi L Talanta 2018, 182, 600–605. [PubMed: 29501199]
(50). Qiao J; Jiang J; Liu L; Shen J; Qi L ACS Appl. Mater. Interfaces 2019, 11, 15133–15140. [PubMed: 30920200]
(51). Ramana P; Schejbal J; Houthoofd K; Martens J; Adams E; Augustijns P; Glatz Z; Van Schepdael A Electrophoresis 2018, 39, 981–988. [PubMed: 29315710]
(52). Li Q-Q; Yang F-Q; Wang Y-Z; Wu Z-Y; Xia Z-N; Chen H Talanta 2018, 185, 16–22. [PubMed: 29759183]
(53). Liu X; Azhar I; Khan H; Qu Q; Tian M; Yang LJ Chromatogr. A 2019, in press 10.1016/j.chroma.2019.460454.
(54). Raza R; Bai Y; Liu H Electrophoresis 2018, 39, 2612–2618. [PubMed: 29775215]
(55). Fayad S; Tannoury M; Morin P; Nehmé R Anal. Chim. Acta 2018, 1020, 134–141. [PubMed: 29655424]
(56). Li Y; Fang H; Hou Z; Sang L; Yang XJ Chromatogr. A 2019, 1591, 171–177.
(57). Ferey J; Da Silva D; Colas C; Nehmé R; Lafite P; Roy V; Morin P; Daniellou R; Agrofoglio L; Maunit B Anal. Chim. Acta 2019, 1049, 115–122. [PubMed: 30612642]
(58). Zhang N; Tian M; Liu X; Yang LJ Chromatogr. A 2018, 1548, 83–91.
(59). Xu M; Zheng M; Liu G; Zhang M; Kang JJ Chromatogr. A 2018, 1537, 128–134.
(60). Wu Z-Y; Zhang H; Li Q-Q; Yang F-Q; Li D-QJ Chromatogr. B 2019, 1110–1111, 67–73.
(61). Chen C; Kramer JS; Brunst S; Proschak E; Scriba GK E. Electrophoresis 2019, 40, 2375–2381.
(62). Farcaş E; Pochet L; Fillet M Talanta 2018, 188, 516–521. [PubMed: 30029407]
(63). Beneito-Cambra M; Gareil P; Badet B; Badet-Denisot M-A; Delaunay NJ Chromatogr. B 2018, 1072, 130–135.
(64). Nguyen TH; Waldrop GL; Gilman SD Electrophoresis 2019, 40, 1558–1564. [PubMed: 30828828]
(65). Yang X; Yan Z; Yu T; Du Y; Chen J; Liu Z; Xi Y Anal. Bioanal. Chem 2018, 410, 5889–5898. [PubMed: 30043111]
(66). Li J; Yu T; Xu G; Du Y; Liu Z; Feng Z; Yang X; Xi Y; Liu JJ Chromatogr. A 2018, 1559, 178–185.
(67). Yang X; Du Y; Feng Z; Liu Z; Li JJ Chromatogr. A 2018, 1559, 170–177.
(68). Ma X; Du Y; Zhu X; Feng Z; Chen C; Yang J Anal. Bioanal. Chem 2019, 411, 5855–5866. [PubMed: 31286176]
(69). Lancioni C; Keunchkarian S; Castells CB; Gagliardi LG J. Chromatogr. A 2018, 1539, 71–77. [PubMed: 29426718]
(70). Yu LX; Amidon G; Khan MA; Hoag SW; Polli J; Raju GK; Woodcock J AAPS J 2014, 16, 771–783. [PubMed: 24854893]
(71). Zhu Q; Scriba GKE J. Pharm. Biomed. Anal 2018, 147, 425–438. [PubMed: 28711220]
(72). Pasquini B; Orlandini S; Villar-Navarro M; Caprini C; Del Bubba M; Douša M; Giuffrida A; Gotti R; Furlanetto SJ Chromatogr. A 2018, 1568, 205–213.
(73). Krait S; Scriba GKE Electrophoresis 2018, 39, 2575–2580. [PubMed: 29600596]
(74). Chalavi S; Fakhari AR; Nojavan S; Mirzaei P Electrophoresis 2018, 39, 2202–2209. [PubMed: 29947135]

(75). Mu Y; Wu X; Huang Y-P; Liu Z-S Electrophoresis 2019, 40, 1992–1995. [PubMed: 31111972]
(76). Ren T; Xu Z Electrophoresis 2018, 39, 1006–1013. [PubMed: 29315662]
(77). Xiao X; Wu J; Li Z; Jia LJ Chromatogr. A 2019, 1587, 14–23.
(78). Pérez-Alcaraz A; Borrull F; Aguilar C; Calull M Electrophoresis 2019, 40, 1762–1770. [PubMed: 31093983]
(79). Šesták J; Theurillat R; Sandbaumhüter FA; Thormann WJ Chromatogr. A 2018, 1558, 85–95.
(80). Gogolashvili A; Tatunashvili E; Chankvetadze L; Sohajda T; Szeman J; Gumustas M; Ozkan SA; Salgado A; Chankvetadze BJ Chromatogr. A 2018, 1571, 231–239.
(81). Bálint M; Darcsi A; Benkovics G; Varga E; Malanga M; Béni S Electrophoresis 2019, 40, 1941–1950. [PubMed: 30892708]
(82). Chu C; Liu C; Jiang L; Lian L; Li J; Li H; Lv H; Yan JJ Sep. Sci 2019, 42, 3009–3015.
(83). Szabó Z-I; Ludmerczki R; Fiser B; Noszál B; Tóth G Electrophoresis 2019, 40, 1897–1903. [PubMed: 30758065]
(84). Varga E; Benkovics G; Darcsi A; Várnai B; Sohajda T; Malanga M; Béni S Electrophoresis 2019, 40, 2789–2798. [PubMed: 31295759]
(85). Sandbaumhüter FA; Thormann W Electrophoresis 2018, 39, 1478–1481. [PubMed: 29572863]
(86). Sursyakova VV; Levdansky VA; Rubaylo AI Electrophoresis 2019, 40, 1656–1661. [PubMed: 30957904]
(87). Chalavi S; Fakhari AR; Nojavan SJ Chromatogr. A 2018, 1567, 211–218.
(88). Zhang Q; Zhang J; Xue S; Rui M; Gao B; Li A; Bai J; yin Z; Anochie EM J. Sep. Sci 2018, 41, 4525–4532. [PubMed: 30307111]
(89). Wang Z; Guo H; Chen M; Zhang G; Chang R; Chen A Electrophoresis 2018, 39, 2195–2201. [PubMed: 29947080]
(90). Greño M; Salgado A; Castro-Puyana M; Marina ML Electrophoresis 2019, 40, 1913–1920. [PubMed: 30892703]
(91). Greño M; Marina ML; Castro-Puyana MJ Chromatogr. A 2018, 1568, 222–228.
(92). Casado N; Salgado A; Castro-Puyana M; García MÁ; Marina ML J. Chromatogr. A 2019, 460407. [PubMed: 31383356]
(93). Trujillo-Rodríguez MJ; Nan H; Varona M; Emaus MN; Souza ID; Anderson JL Anal. Chem 2019, 91, 505–531. [PubMed: 30335970]
(94). Zhang Y; Du Y; Yu T; Feng Z; Chen JJ Pharm. Biomed. Anal 2019, 164, 413–420.
(95). Wahl J; Holzgrabe UJ. Pharm. Biomed. Anal 2018, 148, 245–250. [PubMed: 29059613]
(96). Chu C; Wei M; Liu C; Li H; Cao J; Yan J Anal. Chim. Acta 2018, 1044, 191–197. [PubMed: 30442401]
(97). Zhu C; Li L; Yang G; Irfan M; Wang Z; Fang S; Qu F Talanta 2019, 205 Epub ahead of print 10.1016/j.talanta.2019.06.088.
(98). Kochmann S; Le ATH; Hili R; Krylov SN Electrophoresis 2018, 39, 2991–2996. [PubMed: 30152876]
(99). Lisi S; Fiore E; Scarano S; Pascale E; Boehman Y; Ducongé F; Chierici S; Minunni M; Peyrin E; Ravelet C Anal. Chim. Acta 2018, 1038, 173–181. [PubMed: 30278900]
(100). Ric A; Ecochard V; Iacovoni JS; Boutonnet A; Ginot F; Ong-Meang V; Poinsot V; Paquereau L; Couderc F Anal. Bioanal. Chem 2018, 410, 1991–2000. [PubMed: 29380016]
(101). Le ATH; Krylova SM; Krylov SN Electrophoresis 2019, 40, 2553–2564. [PubMed: 31069842]
(102). Le ATH; Krylova SM; Kanoatov M; Desai S; Krylov SN Angew. Chem., Int. Ed 2019, 58, 2739–2743.
(103). Le ATH; Krylova SM; Krylov SN Anal. Chem 2019, 91, 8532–8539. [PubMed: 31136154]
(104). Beloborodov SS; Krylova SM; Krylov SN Anal. Chem 2019, 91, 12680–12687. [PubMed: 31525943]
(105). Zhang Y; Zhu L; He P; Zi F; Hu X; Wang Q Talanta 2019, 197, 284–290. [PubMed: 30771937]
(106). Zhang Y; Luo F; Zhang Y; Zhu L; Li Y; Zhao S; He P; Wang QJ Chromatogr. A 2018, 1534, 188–194.
(107). Xiao M-W; Bai X-L; Liu Y-M; Yang L; Liao XJ Chromatogr. A 2018, 1569, 222–228.

(108). Sun L; Li Y; Wang H; Zhao Q Talanta 2019, 204, 182–188. [PubMed: 31357280]

(109). Harada S; Hirayama A; Chan Q; Kurihara A; Fukai K; Iida M; Kato S; Sugiyama D; Kuwabara K; Takeuchi A; Akiyama M; Okamura T; Ebbels TMD; Elliott P; Tomita M; Sato A; Suzuki C; Sugimoto M; Soga T; Takebayashi T PLoS One 2018, 13, e0191230. [PubMed: 29346414]

(110). Saoi M; Percival M; Nemr C; Li A; Gibala M; Britz-McKibbin P Anal. Chem 2019, 91, 4709–4718. [PubMed: 30835436]

(111). Huang T; Armbruster M; Lee R; Hui DS; Edwards JL J. Chromatogr. A 2018, 1567, 219–225. [PubMed: 30005940]

(112). Uchitomi R; Hatazawa Y; Senoo N; Yoshioka K; Fujita M; Shimizu T; Miura S; Ono Y; Kamei Y Sci. Rep 2019, 9, 10425. [PubMed: 31320689]

(113). Duncan KD; Lanekoff I Anal. Chem 2019, 91, 7819–7827. [PubMed: 31124661]

(114). Sánchez-López E; Kammeijer GSM; Crego AL; Marina ML; Ramautar R; Peters DJM; Mayboroda OA Sci. Rep 2019, 9, 806. [PubMed: 30692602]

(115). DiBattista A; McIntosh N; Lamoureux M; Al-Dirbashi OY; Chakraborty P; Britz-McKibbin PJ Proteome Res 2019, 18, 841–854.

(116). González-Ruiz V; Gagnebin Y; Drouin N; Codesido S; Rudaz S; Schappler J Electrophoresis 2018, 39, 1222–1232. [PubMed: 29292828]

(117). Saoi M; Sasaki K; Sagawa H; Abe K; Kogiso T; Tokushige K; Hashimoto E; Ohashi Y; Britz-McKibbin PJ Proteome Res. 2019, Epub ahead of print 10.1021/acs.jproteome.9b00405.

(118). Sasaki C; Hiraishi T; Oku T; Okuma K; Suzumura K; Hashimoto M; Ito H; Aramori I; Hirayama Y PLoS One 2019, 14, e0219400. [PubMed: 31295280]

(119). Suzuki M; Yoshioka M; Ohno Y; Akune Y Sci. Rep 2018, 8, 12030. [PubMed: 30104643]

(120). Mori A; Ishikawa K-I; Saiki S; Hatano T; Oji Y; Okuzumi A; Fujimaki M; Koinuma T; Ueno S-I; Imamichi Y; Hattori N PLoS One 2019, 14, e0223113. [PubMed: 31560709]

(121). Zhang W; Segers K; Mangelings D; Van Eeckhaut A; Hankemeier T; Vander Heyden Y; Ramautar R Electrophoresis 2019, 40, 2309–2320. [PubMed: 31025710]

(122). MacLennan MS; Kok MGM; Soliman L; So A; Hurtado-Coll A; Chen DDY J. Chromatogr. B 2018, 1074–1075, 79–85.

(123). Cieslarova Z; Magaldi M; Barros LA; do Lago CL; Oliveira DR; Fonseca FAH; Izar MC; Lopes AS; Tavares MFM; Klassen AJ Chromatogr. A 2019, 1583, 136–142.

(124). Moldovan R-C; Bodoki E; Servais A-C; Chankvetadze B; Crommen J; Oprean R; Fillet MJ Chromatogr. A 2018, 1564, 199–206.

(125). Yatsuoka W; Ueno T; Miyano K; Uezono Y; Enomoto A; Kaneko M; Ota S; Soga T; Sugimoto M; Ushijima T PLoS One 2019, 14, e0220712. [PubMed: 31404085]

(126). Binek A; Rojo D; Godzien J; Rupérez FJ; Nuñez V; Jorge I; Ricote M; Vázquez J; Barbas CJ Proteome Res. 2019, 18, 169–181.

(127). Kelley ZD; Rogers DT; Littleton JM; Lynn BC Electrophoresis 2019, Early View 10.1002/elps.201900220.

(128). Portero EP; Nemes P Analyst 2019, 144, 892–900. [PubMed: 30542678]

(129). Zhang W; Guled F; Hankemeier T; Ramautar RJ Chromatogr. B 2019, 1105, 10–14.

(130). Liu Z; Portero EP; Jian Y; Zhao Y; Onjiko RM; Zeng C; Nemes P Anal. Chem 2019, 91, 5768–5776. [PubMed: 30929422]

(131). Drouin N; Pezzatti J; Gagnebin Y; González-Ruiz V; Schappler J; Rudaz S Anal. Chim. Acta 2018, 1032, 178–187. [PubMed: 30143215]

(132). Masumoto H; Matsuyama S PLoS One 2018, 13, e0194942. [PubMed: 29579121]

(133). Villaseñor A; Aedo-Martín D; Obeso D; Erjavec I; Rodríguez-Coira J; Buendía I; Ardura JA; Barbas C; Gortazar AR Sci. Rep 2019, 9, 2295. [PubMed: 30783155]

(134). Tubaon RM; Haddad PR; Quirino JP Anal. Chem 2018, 90, 10122–10127. [PubMed: 30074774]

(135). Azab S; Ly R; Britz-McKibbin P Anal. Chem 2019, 91, 2329–2336. [PubMed: 30570251]

(136). Kawai T; Ota N; Okada K; Imasato A; Owa Y; Morita M; Tada M; Tanaka Y Anal. Chem 2019, 91, 10564–10572. [PubMed: 31357863]

(137). Kawai T; Ota N; Imasato A; Shirasaki Y; Otsuka K; Tanaka YJ Chromatogr. A 2018, 1565, 138–144.

(138). Khan S; Liu J; Szabo Z; Kunnummal B; Han X; Ouyang Y; Linhardt RJ; Xia Q Rapid Commun. Mass Spectrom 2018, 32, 882–888. [PubMed: 29575162]

(139). Reider B; Szigeti M; Guttman A Talanta 2018, 185, 365–369. [PubMed: 29759213]

(140). Borza B; Szigeti M; Szekrenyes A; Hajba L; Guttman AJ Pharm. Biomed. Anal 2018, 153, 182–185.

(141). Cowper B; Li X; Yu L; Zhou Y; Fan WH; Rao CM J. Pharm. Biomed. Anal 2018, 153, 214–220. [PubMed: 29502007]

(142). Szigeti M; Chapman J; Borza B; Guttman A Electrophoresis 2018, 39, 2340–2343. [PubMed: 29600574]

(143). Bruneel A; Cholet S; Drouin-Garraud V; Jacquemont M-L; Cano A; Mégarbané A; Ruel C; Cheillan D; Dupré T; Vuillaumier-Barrot S; Seta N; Fenaille F Electrophoresis 2018, 39, 3123–3132. [PubMed: 29869806]

(144). Rossdam C; Konze SA; Oberbeck A; Rapp E; Gerardy-Schahn R; von Itzstein M; Buettner FFR Anal. Chem 2019, 91, 6413–6418. [PubMed: 31058489]

(145). Lu G; Holland LA Anal. Chem 2019, 91, 1375–1383. [PubMed: 30525457]

(146). Song W; Zhou X; Benktander JD; Gaunitz S; Zou G; Wang Z; Novotny MV; Jacobson SC Anal. Chem 2019, 10.1021/acs.analchem.1029b02620.

(147). Lageveen-Kammeijer GSM; de Haan N; Mohaupt P; Wagt S; Filius M; Nouta J; Falck D; Wuhrer M Nature Commun. 2019, 10, 2137. [PubMed: 31086181]

(148). Jooß K; Meckelmann SW; Klein J; Schmitz OJ; Neusüß C Anal. Bioanal. Chem 2019, 411, 6255–6264. [PubMed: 30535529]

(149). Haselberg R; De Vijlder T; Heukers R; Smit MJ; Romijn EP; Somsen GW; Domínguez-Vega E Anal. Chim. Acta 2018, 1044, 181–190. [PubMed: 30442400]

(150). Giorgetti J; D'Atri V; Canonge J; Lechner A; Guillarme D; Colas O; Wagner-Rousset E; Beck A; Leize-Wagner E; François Y-N Talanta 2018, 178, 530–537. [PubMed: 29136858]

(151). Szarka M; Szigeti M; Guttman A Anal. Chem 2019, 91, 7738–7743. [PubMed: 31136147]

(152). Sanderson P; Stickney M; Leach FE; Xia Q; Yu Y; Zhang F; Linhardt RJ; Amster IJ J. Chromatogr. A 2018, 1545, 75–83. [PubMed: 29501428]

(153). Stickney M; Sanderson P; Leach FE; Zhang F; Linhardt RJ; Amster IJ Int. J. Mass Spectrom 2019, 445, 116209.

(154). Ouyang Y; Han X; Xia Q; Chen J; Velagapudi S; Xia K; Zhang Z; Linhardt RJ Anal. Chem 2019, 91, 846–853. [PubMed: 30516363]

(155). Saar KL; Müller T; Charmet J; Challa PK; Knowles TPJ Anal. Chem 2018, 90, 8998–9005. [PubMed: 29938505]

(156). Zhou W; Xia L; Xiao X; Li G; Pu Q Electrophoresis 2019, 40, 2165–2171. [PubMed: 30861170]

(157). Saar KL; Zhang Y; Müller T; Kumar CP; Devenish S; Lynn A; Łapińska U; Yang X; Linse S; Knowles TPJ Lab Chip 2018, 18, 162–170.

(158). Dutta D Electrophoresis 2018, 39, 760–769. [PubMed: 29115696]

(159). Kochmann S; Krylov SN Anal. Chem 2018, 90, 9504–9509. [PubMed: 29969016]

(160). Arter WE; Charmet J; Kong J; Saar KL; Herling TW; Müller T; Keyser UF; Knowles TPJ Anal. Chem 2018, 90, 10302–10310. [PubMed: 30070105]

(161). Wang S; Zhang L; Sun H; Chu Z; Chen H; Zhao Y; Zhang W Electrophoresis 2019, 40, 2610–2617. [PubMed: 30977523]

(162). Höving S; Janasek D; Novo P Anal. Chim. Acta 2018, 1044, 77–85. [PubMed: 30442407]

(163). Pfeiffer SA; Rudisch BM; Glaeser P; Spanka M; Nitschke F; Robitzki AA; Schneider C; Nagl S; Belder D Anal. Bioanal. Chem 2018, 410, 853–862. [PubMed: 29085988]

(164). Rudisch BM; Pfeiffer SA; Geissler D; Speckmeier E; Robitzki AA; Zeitler K; Belder D Anal. Chem 2019, 91, 6689–6694. [PubMed: 31034207]

(165). Ivanov NA; Liu Y; Kochmann S; Krylov SN Lab Chip 2019, 19, 2156–2160. [PubMed: 31161184]

(166). Höcker O; Montealegre C; Neusüß C Anal. Bioanal. Chem 2018, 410, 5265–5275. [PubMed: 29943266]

(167). Beutner A; Piendl SK; Wert S; Matysik F-M Anal. Bioanal. Chem 2018, 410, 6321–6330. [PubMed: 30027317]

(168). González-Ruiz V; Codesido S; Rudaz S; Schappler J Electrophoresis 2018, 39, 853–861. [PubMed: 29124762]

(169). Sasaki K; Sagawa H; Suzuki M; Yamamoto H; Tomita M; Soga T; Ohashi Y Anal. Chem 2019, 91, 1295–1301. [PubMed: 30500154]

(170). Krenkova J; Kleparnik K; Luksch J; Foret F Electrophoresis 2019, 40, 2263–2270. [PubMed: 30794321]

(171). Konášová R; Koval D; Dytrtová JJ; Kašička VJ Chromatogr. A 2018, 1568, 197–204.

(172). Hirayama A; Abe H; Yamaguchi N; Tabata S; Tomita M; Soga T Electrophoresis 2018, 39, 1382–1389. [PubMed: 29493797]

(173). Scholl T; Dietze C; Schmidt M; Ohla S; Belder D Anal. Bioanal. Chem 2018, 410, 5741–5750. [PubMed: 29974150]

(174). Shen Y; Zhao X; Wang G; Chen DDY Anal. Chem 2019, 91, 3805–3809. [PubMed: 30830762]

(175). Shi M; Huang Y; Zhao J; Li S; Liu R; Zhao S Talanta 2018, 179, 466–471. [PubMed: 29310261]

(176). Fu Y-J; Chen L; Guo X-F; Wang H Electrophoresis 2019, 40, 1027–1033. [PubMed: 30653681]

(177). Chadha R; Kalminskii G; Tierney AJ; Knopf JD; Lazo de la Vega L; McElrath B; Kovarik ML Anal. Chem 2018, 90, 11344–11350. [PubMed: 30175919]

(178). Proctor A; Allbritton NL Analyst 2019, 144, 961–971. [PubMed: 30207332]

(179). Pan Q; Yamauchi KA; Herr AE Anal. Chem 2018, 90, 13419–13426. [PubMed: 30346747]

(180). Sinkala E; Rosàs-Canyelles E; Herr AE Analyst 2019, 144, 972–979. [PubMed: 30234203]

(181). Lu S; Dugan CE; Kennedy RT Anal. Chem 2018, 90, 5171–5178. [PubMed: 29578696]

(182). Marczak S; Richards K; Ramshani Z; Smith E; Senapati S; Hill R; Go DB; Chang H-C Electrophoresis 2018, 39, 2029–2038.

(183). van Tricht E; Geurink L; Galindo Garre F; Schenning M; Backus H; Germano M; Somsen GW; C. E. Sänger – van de Griend Electrophoresis 2019, 40, 2277–2284. [PubMed: 30951206]

(184). Michen B; Graule TJ Appl. Microbiol 2010, 109, 388–397.

(185). Loughney JW; Minsker K; Ha S; Rustandi RR Electrophoresis 2019, 40, 2602–2609. [PubMed: 31218707]

(186). Li F; Macdonald NP; Guijt RM; Breadmore MC Anal. Chem 2019, 91, 1758–1763. [PubMed: 30513198]

(187). Gong H; Bickham BP; Woolley AT; Nordin GP Lab Chip 2017, 17, 2899–2909. [PubMed: 28726927]

(188). Beauchamp MJ; Nielsen AV; Gong H; Nordin GP; Woolley AT Anal. Chem 2019, 91, 7418–7425. [PubMed: 31056901]

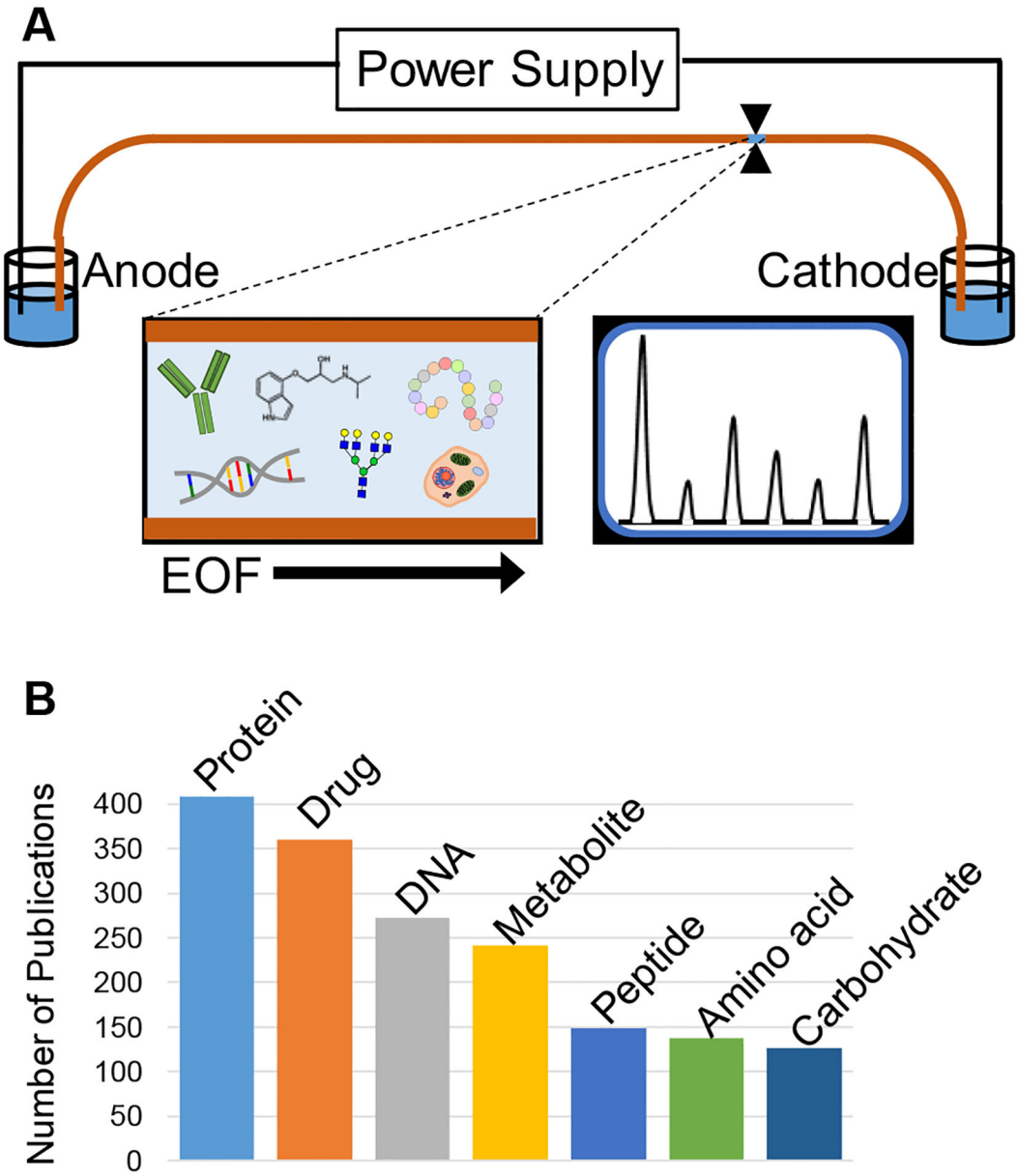

Figure 1.

(A) is a conceptual depiction of biomolecular analyses with CE. (B) summarizes the results of a search using the SciFinder Scholar® database to estimate the frequency of publications from January 2018 through October 2019 that contained the term capillary electrophoresis and the biomolecular classes listed in the figure.

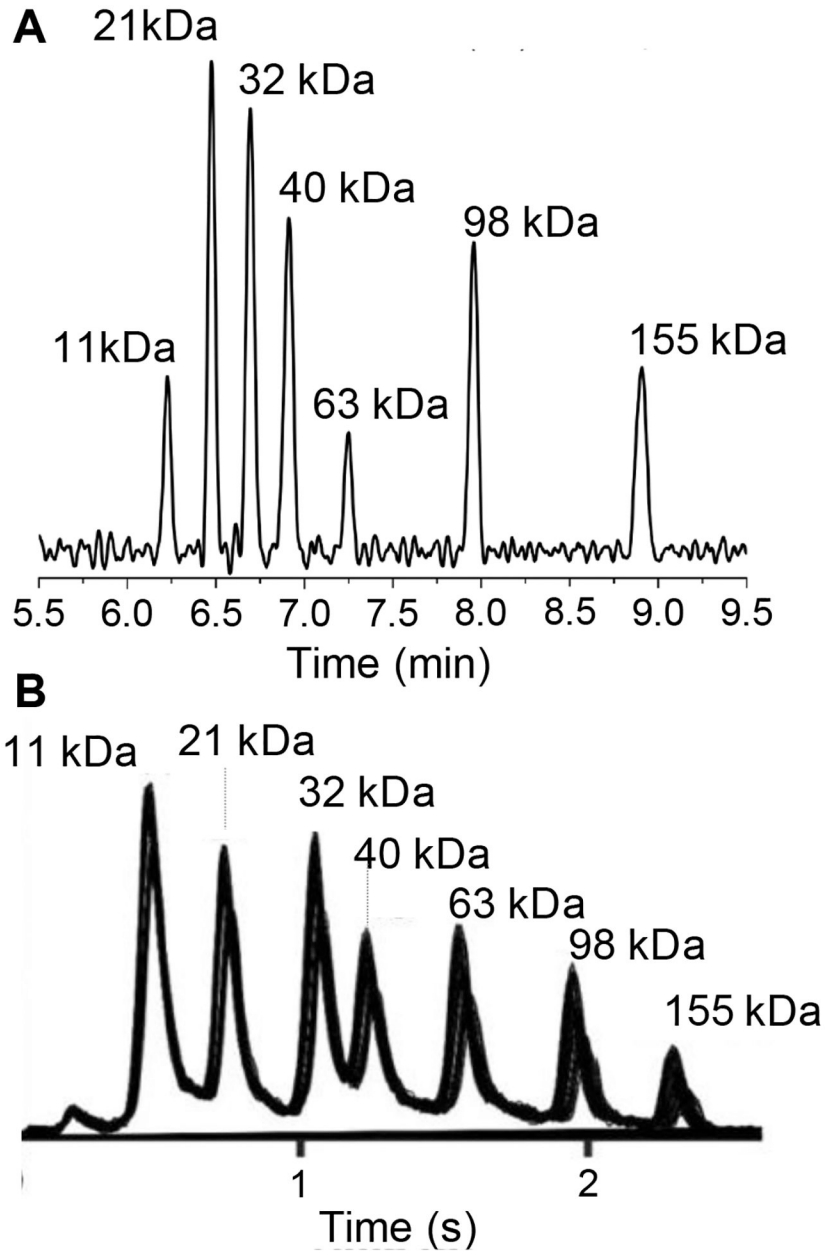

Figure 2.

illustrates the utility of CE for protein separations under conditions of high efficiency and high throughput. (A) depicts size-based sieving of the Benchmark protein size standard separated with packed capillary electrophoresis utilizing colloidal silica particles as the packing material. (B) depicts the separation of a protein standard using SDS and a physical gel composed of a polymer. (A) Adapted with permission from Electrophoresis of megaDalton proteins inside colloidal silica, Ragland, T.S.; Gossage, M.D.; Furtaw, M.D.; Anderson, J.P.; Steffens, D.L.; Wirth, M.J. Electrophoresis. Vol. 40, Issue 5 (ref 7). Copyright 2019 Wiley. (B) Adapted by permission from Springer, Anal. Bioanal. Chem., Vol. 411 pp. 6155–6163, Droplet sample introduction to microchip gel and zone

electrophoresis for rapid analysis of protein-protein complexes and enzymatic reactions, Ouimet, C.M., C.I. D'Amico, and R.T. Kennedy (ref 8). Copyright 2019.

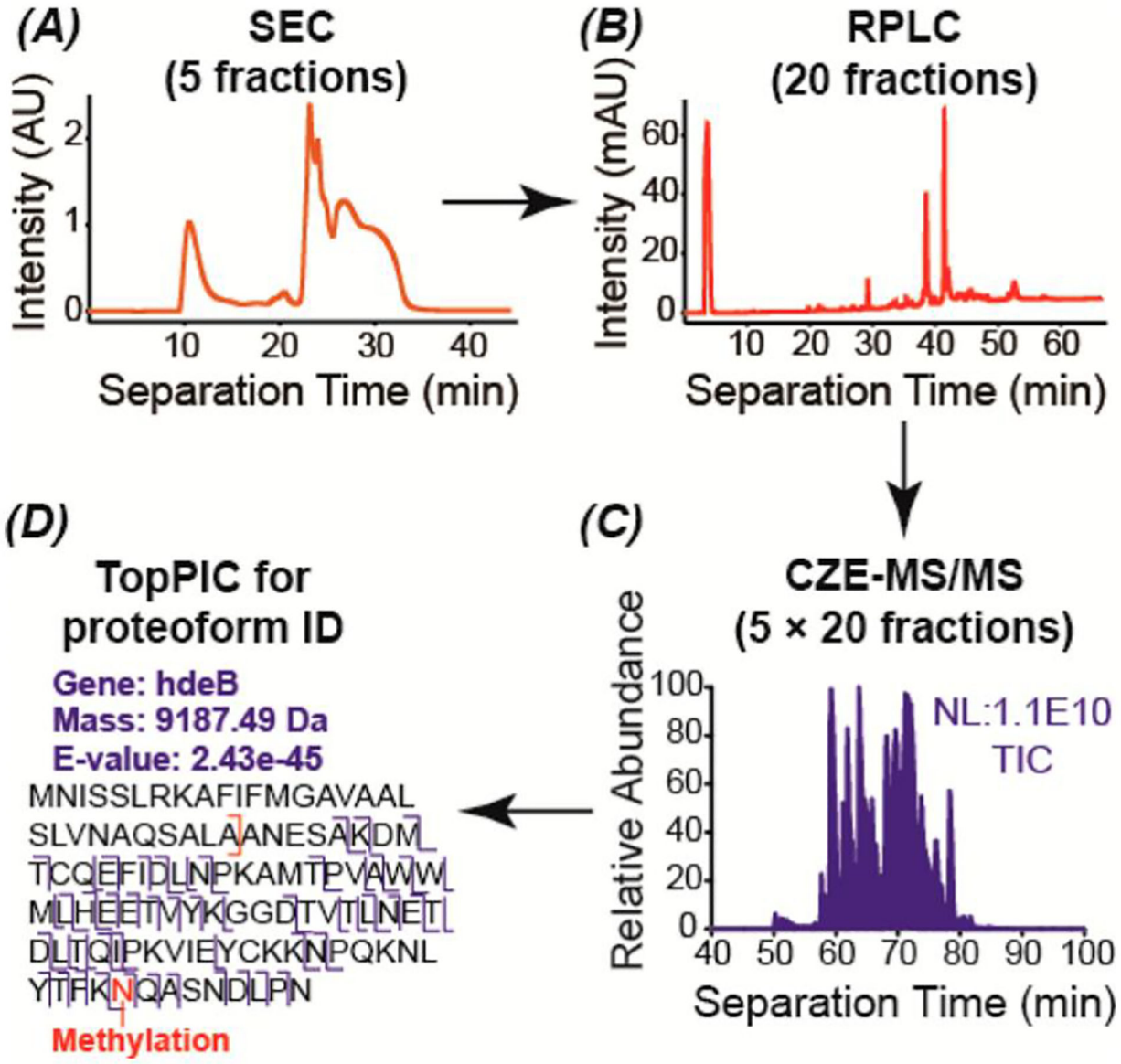

Figure 3.

illustrates a multi-dimensional separation platform that incorporates capillary electrophoresis to increase the identification of proteins and proteoforms. (A) size exclusion chromatography chromatogram. (B) chromatogram using reversed phase liquid chromatography. (C) Total ion current chromatogram after CE-MS/MS. (D) fragmentation pattern of an identified proteoform using TopPIC software. Reprinted with permission from McCool, E. N.; Lubeckyj, R. A.; Shen, X.; Chen, D.; Kou, Q.; Liu, X.; Sun, L. Anal. Chem. 2018, 90, 5529–5533 (ref 19). Copyright 2018 American Chemical Society.

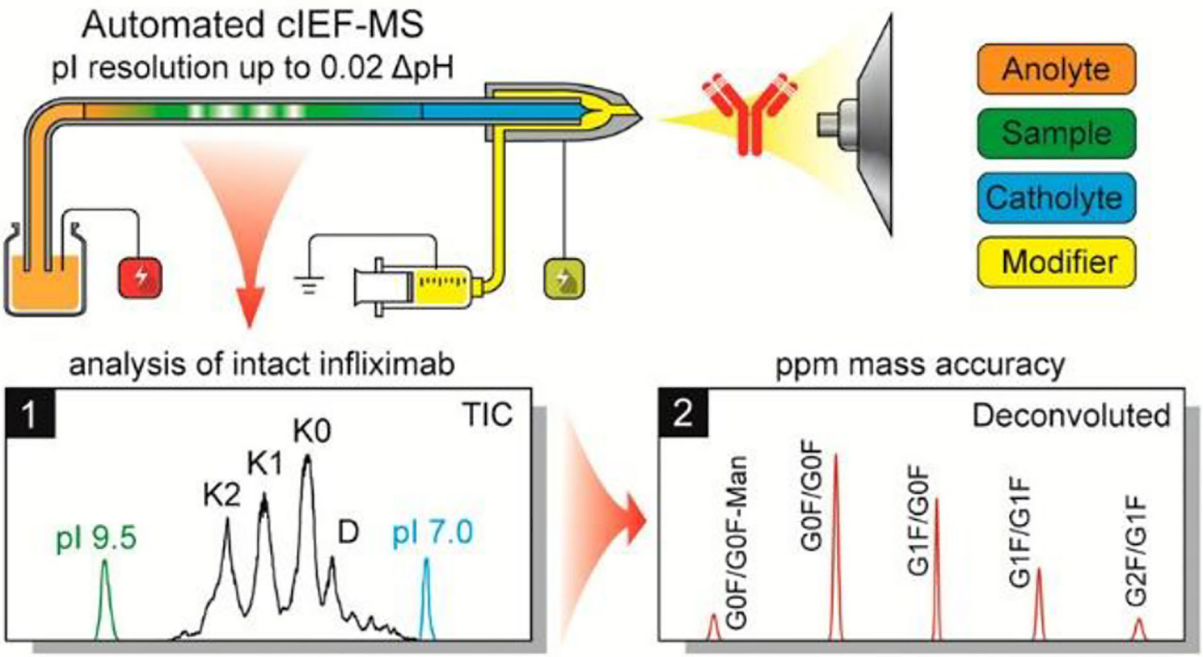

Figure 4.

illustrates an automated platform coupling capillary isoelectric focusing and high resolution mass spectrometry for antibody and protein analyses. The automated platform can provide structural information and isoelectric points. Reprinted with permission from Wang, L.; Bo, T.; Zhang, Z.; Wang, G.; Tong, W.; Da Yong Chen, D. Anal Chem. 2018, 90, 9495–9503 (ref 33). Copyright 2018 American Chemical Society.

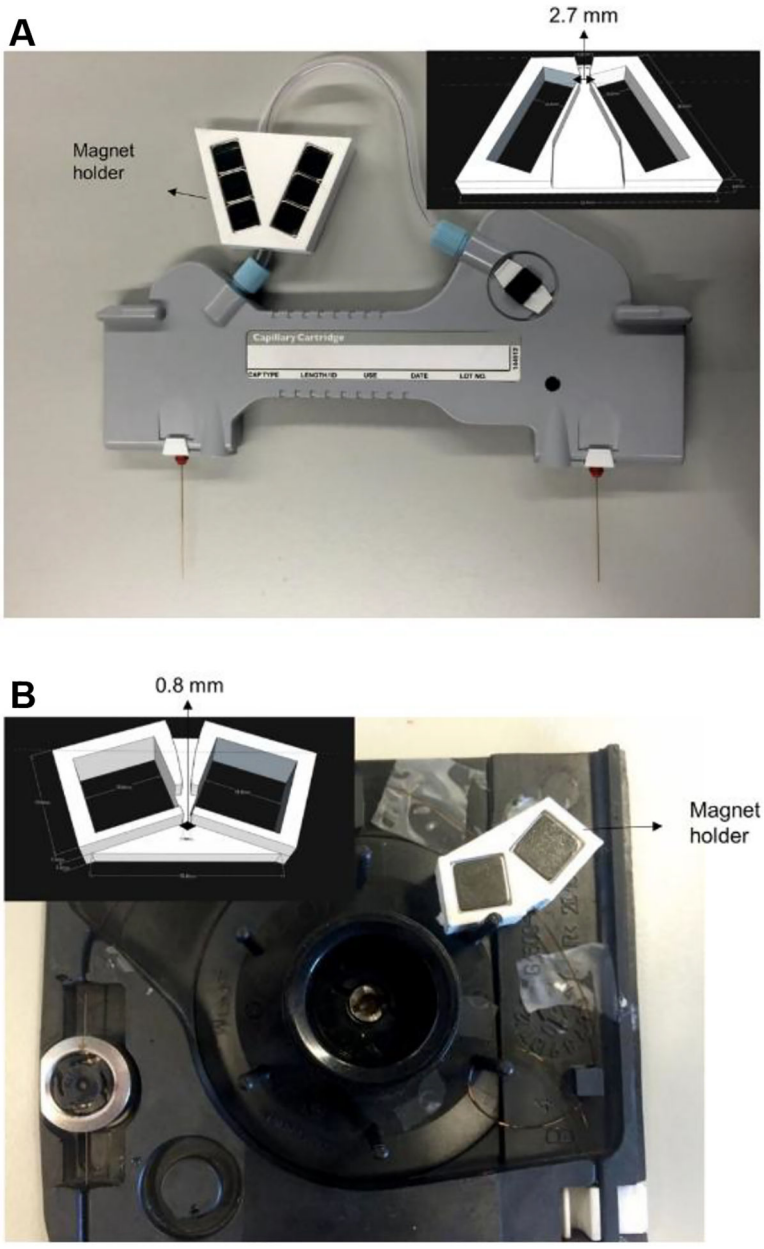

Figure 5.

illustrates a 3D printed magnet holder for (A) a liquid based cooled commercial capillary electrophoresis instrument and for (B) an air based cooled capillary system for the control of magnetic microparticles in immobilized enzymatic assays performed on-line. Reproduced with permission from An improved design to capture magnetic microparticles for capillary electrophoresis based immobilized microenzyme reactors, Ramana, P.; Schejbal, J.; Houthoofd, K.; Martens, J.; Adams, E.; Augustijns, P.; Glatz, Z.; Schepdael, A. V. Electrophoresis., Vol. 39, (ref 51). Copyright 2018 Wiley

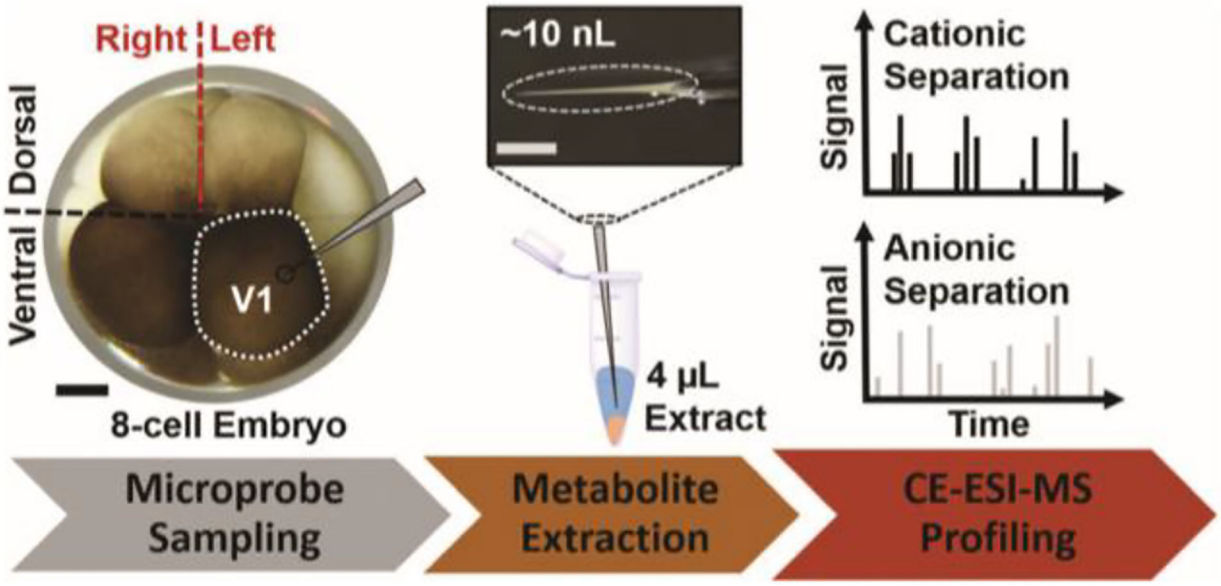

Figure 6.

depicts a capillary electrophoresis-electrospray ionization-mass spectrometry platform for the identification of anionic and cationic species from a live embryonic frog cell. The left ventricle, V1, of the cell was identified using a 10 nL portion of its cellular content for analysis. Reproduced from Portero, E.P.; Nemes, P. Analyst 2019, 144, 892–900 (ref 128), with permission of The Royal Society of Chemistry.

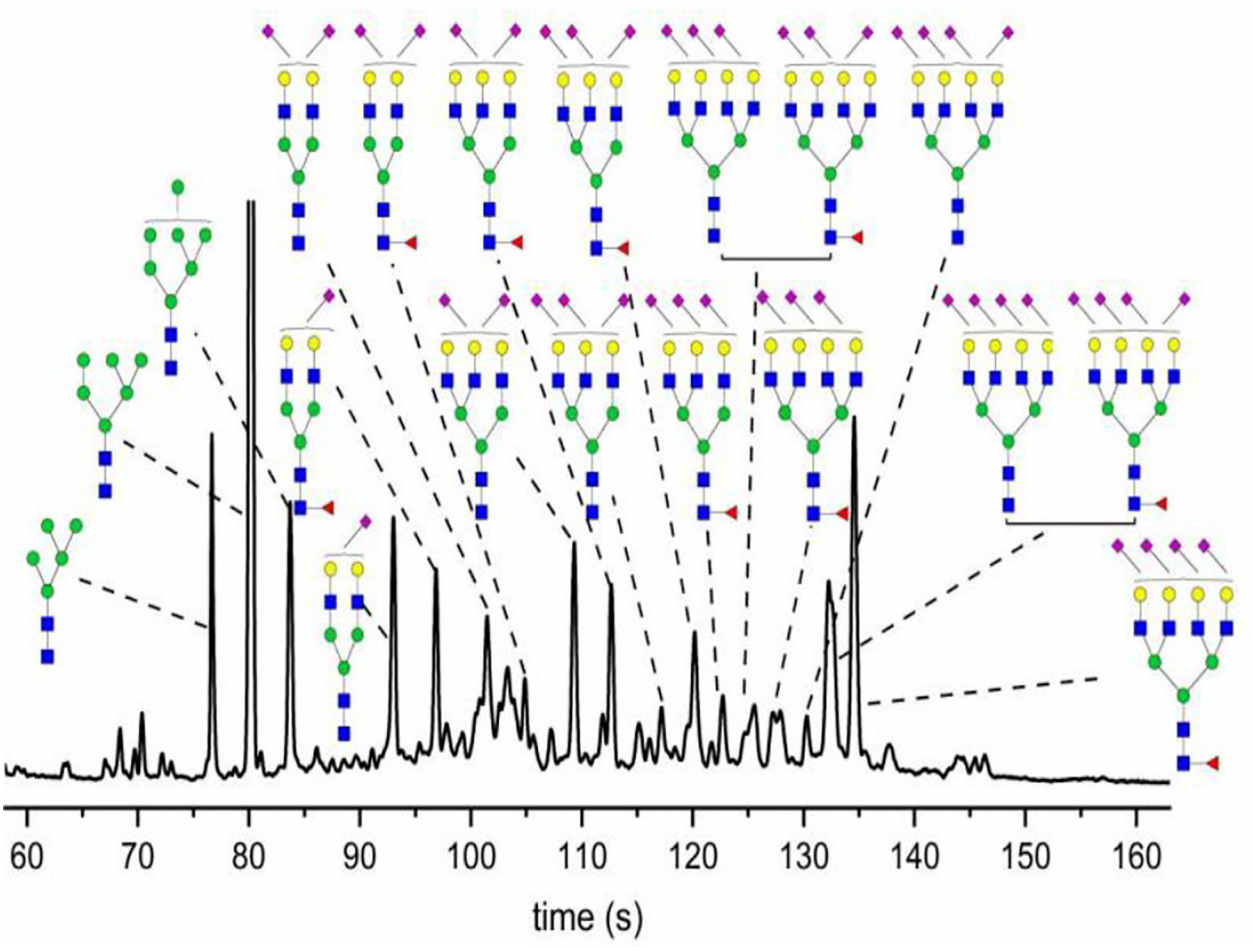

Figure 7.

is an electropherogram of N-glycans with α2–3 and α2–6 linked sialic acids from human urinary exosomes. The trace is obtained using microfluidic electrophoresis. Reproduced from Song, W.; Zhou, X.; Benktander, J.D.; Gaunitz, S.; Zou, G.; Wang, Z.; Novotny, M.V.; Jacobson, S.C. Anal. Chem. 2019, (ref 146). Copyright 2019 American Chemical Society.

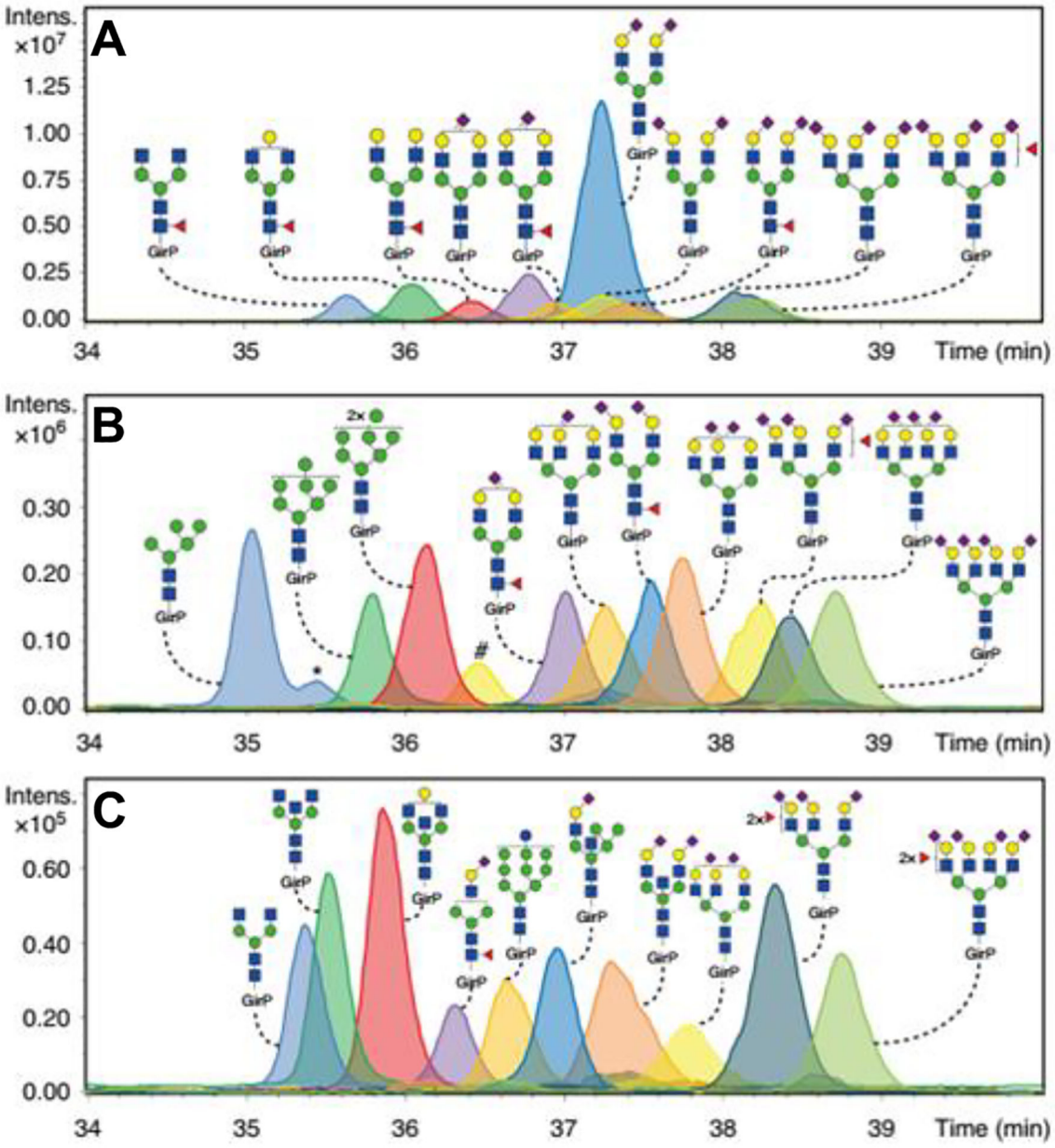

Figure 8.

is an electropherogram of N-glycans with α2–3 and α2–6 linked sialic acids from human plasma. The traces are obtained using CE-MS. The upper trace (A) is of N-glycans at high abundance (> 2%). The middle trace (B) is of intermediate abundance (from 0.5% to 1%). The lower trace (C) is of N-glycans at low abundance (< 0.25%). Adapted by permission from Macmillan Publishers Ltd: Nature Communications, Lageveen-Kammeijer, G. S.M.; de Haan, N.; Mohaupt, P.; Wagt, S.; Filius, M.; Nouta, J.; Falck, D.; Wuhrer, M., Nature Communications 2019, 10(1), 2137 (ref #147). Copyright 2019. <https://www.nature.com/articles/s41467-019-09910-7≥

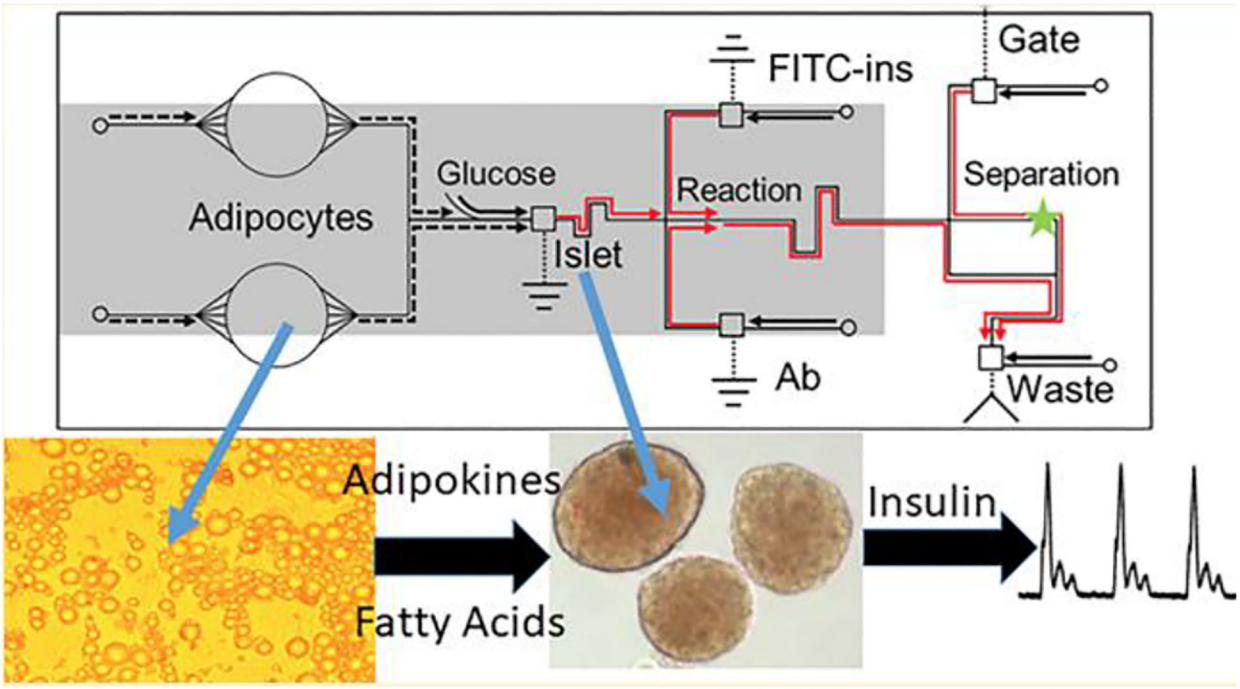

Figure 9.

depicts the layout of a microfluidic device capable of modeling in vivo circulation to investigate cell-cell interactions. Coupled with electrophoresis, this body-on-chip microfluidic device was used to investigate the effects of adipocytes on insulin secretion from islets of Langerhans. Reproduced from Lu, S.; Dugan, C.E.; Kennedy, R.T. Anal. Chem. 2018. 90(8), 5171–5178 (ref 181). Copyright 2018 American Chemical Society.

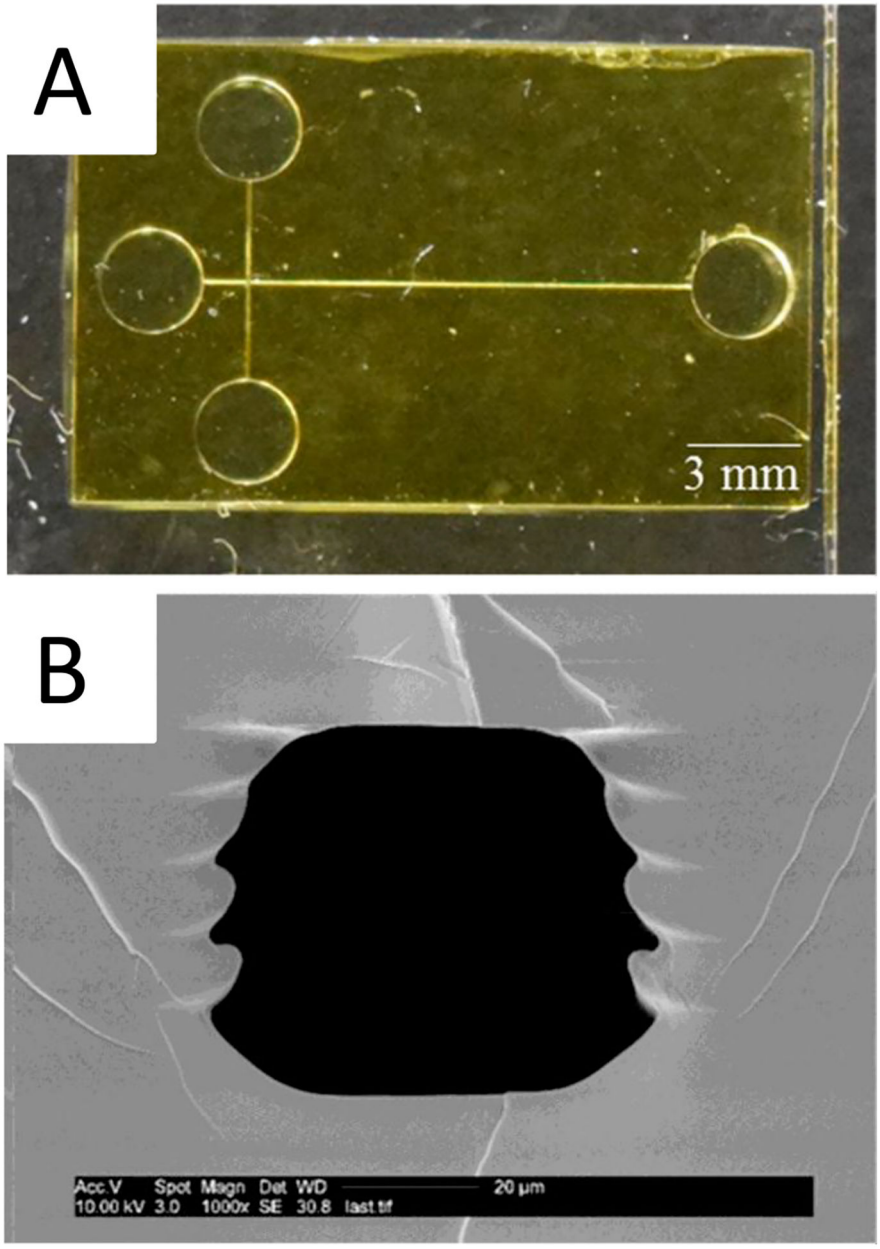

Figure 10.
is an image of (A) a 3D printed microfluidic device. (B) contains an SEM image of a channel cross section. Adapted from Beauchamp, M. J.; Nielsen, A. V.; Gong, H.; Nordin, G. P.; Woolley, A. T., Anal Chem. 2019, 91 (11), 7418–7425 (ref 188). Copyright 2019 American Chemical Society.